QJEGH

Research article

Quarterly Journal of Engineering Geology and Hydrogeology

https://doi.org/10.1144/qjegh2023-160 | Vol. 58 | 2025 | qjegh2023-160

Enhancing the visualization and analysis of geotechnical properties: examples from the 3D volume change potential of UK clay soils

L. D. Jones*, R. Terrington and A. Hulbert

British Geological Survey, Nicker Hill, Keyworth, Nottingham NG12 5GG, UK

LDJ, 0000-0003-4825-7238; RT, 0000-0002-7594-1441; AH, 0009-0001-6923-1662

*Correspondence: ldjon@bgs.ac.uk

Abstract: Ground shrinkage due to shrink–swell clay soils is the most damaging geohazard in the UK, costing the economy an estimated £3.4 billion over the past 10 years. The towns, cities and infrastructure most susceptible to this shrink–swell behaviour are found mainly in the SE of the country. Ten of these clay-rich soils have been used in this study. The volume change potential (VCP) of a soil is the relative change in volume to be expected with changes in the soil moisture content, and is reflected by the shrinking and swelling of the ground. Variations in plasticity with area and with depth can be depicted using purely statistical methods. To construct a more representative model of spatial VCP variations in clay-rich formations a more sophisticated 3D interpolation is required such as lithofacies modelling, which can be used to produce multiple realizations of the variation of parameters (e.g. lithology) across a domain where there is an abundance of *XYZ* data from boreholes or point samples. Virtalis GeoVisionary software provides a means of viewing the lithofacies-type generated data in a fully immersive 3D environment. Similar visualization can be carried out against many environmental parameters and geoscience datasets such as, for example, borehole, geophysical data, point clouds and CAD models. Voxel models are easily imported and are able to be visualized in their 'true' spatial position, overlying geology or standard maps. The Geosure Shrink–Swell 3D dataset, created using Esri ArcGIS, provides a regional susceptibility model of the potential shrink–swell hazard in the London and Thames Valley area. 2D representations based on statistical analyses show general trends; but with large amounts of data unevenly spread over a wide area, the detail is lost. 3D models, such as those created using voxelated facies techniques, provide a seamless interpolation and deliver a visualization of VCP that can be interpreted across a variety of depths.

This paper builds on work presented previously by the first two authors of this paper, in Volume 44 of *QJEGH*, in two ways: first, it expands on the scope of the work, adding nine more clay soils to that of the previously reported London Clay; and, secondly, it builds and improves on the use and type of visualization and analysis undertaken to model them.

Received 18 December 2023; **revised** 28 March 2025; **accepted** 12 May 2025

Many towns, cities, transport routes and buildings are founded on clay-rich soils and rocks in the UK. The clays within these materials may be a significant hazard to engineering construction due to their ability to shrink or swell with seasonal changes in moisture content (often related to rainfall and the evapotranspiration of vegetation), local site changes such as leakage from water supply pipes or drains, changes to surface drainage and landscaping (including paving), or following the planting, removal or severe pruning of trees or hedges.

In the UK, the effects of shrinkage and swelling of clay soils, with respect to foundation and building damage, were first recognized by geotechnical specialists following the dry summer of 1947, and since then the cost of damage due to shrinking and swelling clay soils has risen dramatically. Over the past 10 years the adverse effects of shrink–swell behaviour has cost the economy an estimated £3 billion, making it the most damaging geohazard in Britain today (Jones and Jefferson 2012). The Association of British Insurers has estimated that the average cost of shrink–swell-related subsidence to the insurance industry stands at over £400 million a year (Driscoll and Crilly 2000), and that by 2050 this could rise to over £600 million.

Engineering geologists at the British Geological Survey (BGS) have been investigating the geotechnical and mineralogical factors controlling volume change behaviour of UK clay soils and mudrocks for over 20 years. Formations studied include the Gault Clay Formation (Forster *et al.* 1994; Jones and Hobbs 1998*a*), the Mercia Mudstone Group (Jones and Hobbs 1998*b*; Hobbs *et al.* 2002), the Lambeth Group (Jones 2001; Jones and Hobbs 2004), the Lias Group (Hobbs *et al.* 2012), the London Clay Formation (Jones and Terrington 2011) and the Wealden Group (Freeborough *et al.* 2011).

In the UK, towns and cities built on clay-rich soils most susceptible to shrink–swell behaviour are found mainly in the SE of the country, 10 of these clay-rich soils have been used in this study (Fig. 1). In these areas many of the 'clay' formations are too young to have been changed into stronger 'mudstones', leaving them still able to absorb and lose moisture. Clay rocks elsewhere in the country are older and have been hardened by processes resulting from deep burial and so are less able to absorb water. The clay soils in this paper are both relatively young clays (e.g. London Clay), weak to very weak mudstones (e.g. Mercia Mudstone) or interbedded mudstones (e.g. Lias). Some areas (e.g. around The Wash and under the Lancashire Plain) are deeply buried beneath other (superficial) soils that are not susceptible to shrink–swell behaviour. However, other superficial deposits such as alluvium, peat and laminated clays can also be susceptible to soil subsidence and heave (e.g. in the Vale of York and the Cheshire Basin). The depth to which shrinkage and swelling occurs is usually confined to the active zone (upper 1.5 m) where moisture change and weathering processes are most likely to occur, unless this zone is extended by the presence of tree roots (Driscoll 1983).

In the UK, some Mesozoic and Neogene–Paleogene (Tertiary) clay soils and weak mudrocks, including the London Clay Formation, are susceptible to shrinkage and swelling as environmental conditions change (Harrison *et al.* 2012). Indications are that climate change will have an increasingly adverse effect on the

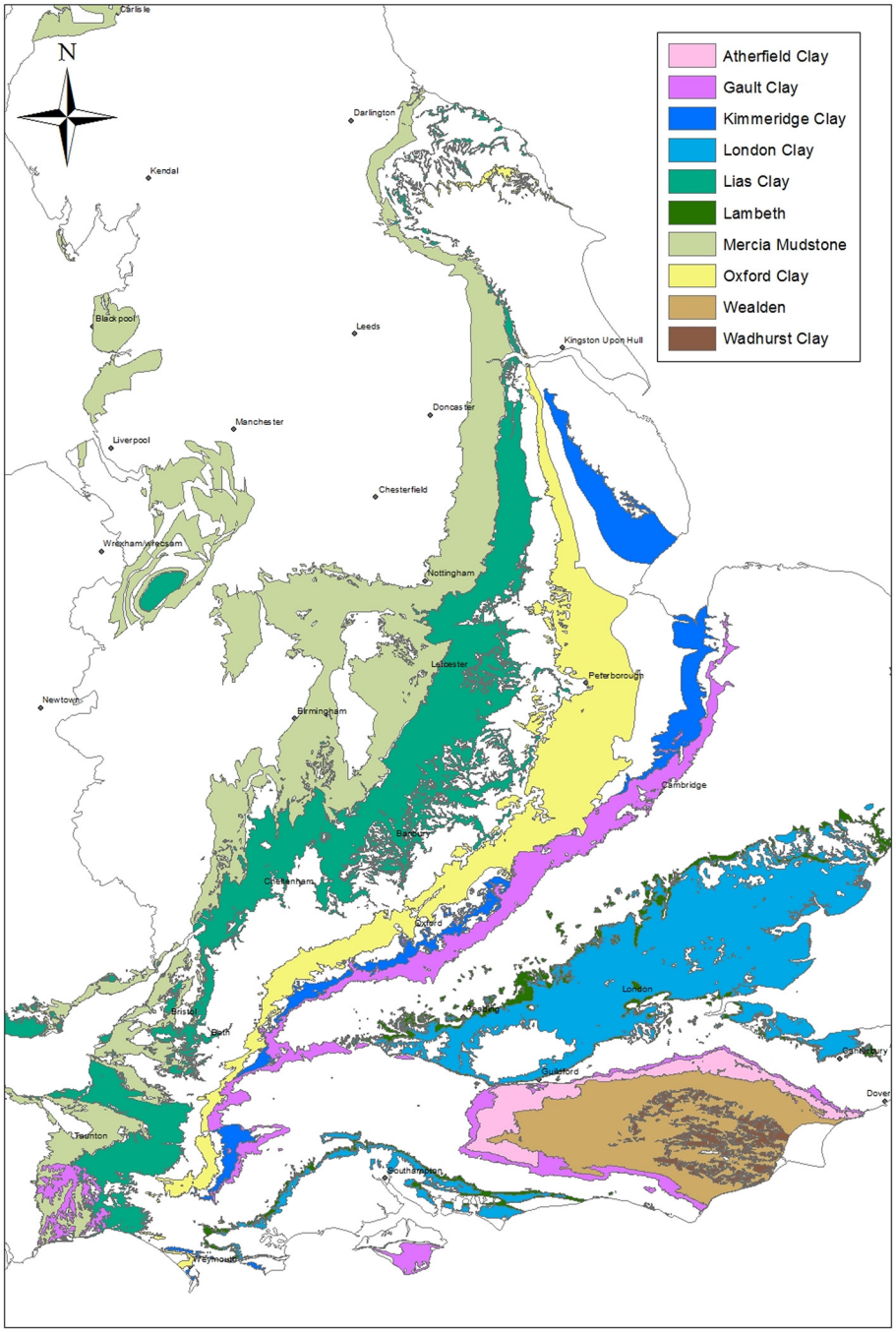

Fig. 1. Distribution of UK clay-rich soil formations used in this study (shown in alphabetical order).

moisture conditions that UK soils experience, and therefore on the damage caused to homes, buildings and roads. The government has recognized that climate change is one of the biggest problems that the UK faces and, if current predictions are correct, we can expect hotter, drier summers in the SE of England, including the areas underlain by these clay-rich soils, and milder, wetter winters in the rest of the UK (Met Office 2018). The shrink–swell process is controlled by temperature and the amount of rainfall, and their distribution throughout the year. It also depends on the amount of expansive clay minerals in the soil; the more expansive clay minerals, such as smectite, it contains, the higher its swell potential and the more water it can absorb. The change in the amount and distribution of rainfall, as a result of climate change, will lead to a significant increase in the damage done by the shrinking and swelling behaviour of these clay soils. In fact, as many as one in five homes in England and Wales are likely to be damaged by ground that swells when it gets wet and shrinks as it dries out (Jones 2004). If the UK were to experience an increase in extended periods of dry weather, prior to future rainfall events, costs could rise significantly.

Formation information

The basic geotechnical properties and mineralogy of the major clay-rich formations in the UK are well known, and are well documented throughout the published literature. Therefore, it was determined that it would be unnecessary to add to this. However, onshore subcrop, outcrop and total area coverage of Great Britain (based on the BGS 1:250 000 digital geology map – DigMap 250k) for the 10 formations are given in Table 1, along with some useful references detailing their typical engineering descriptions, geology and mineralogy.

Volume change potential

The volume change potential (VCP) of a soil is the relative change in volume to be expected with changes in the soil moisture content

Table 1. Formation information (in alphabetical order)

Formation	Onshore subcrops (km^2)	Outcrop (km^2)	UK area (%)	References for typical:	
				engineering description	geology and mineralogy
Atherfield Clay (AC)	72	51	<0.1	Hopson *et al.* (2008)	Simpson (1985)
Gault Clay (GLT)	1441	785	0.7	Forster *et al.* (1994)	Hopson *et al.* (2001)
Kimmeridge Clay (KC)	2609	642	1.2	Reeves *et al.* (2006)	Horton *et al.* (1995)
Lambeth Group (LMBE)	986	351	0.5	Jones and Hobbs (2004)	Ellison *et al.* (1994)
Lias Clay (LIAS)	8566	4675	4.1	Hobbs *et al.* (2012)	Cox *et al.* (1999)
London Clay (LC)	6493	2245	3.1	Jones and Terrington (2011)	King (1981)
Mercia Mudstone Group (MMG)	11 999	3818	5.7	Hobbs *et al.* (2002)	Howard *et al.* (2008)
Oxford Clay (OXC)	4290	1324	2.0	Reeves *et al.* (2006)	Cox *et al.* (1992)
Wadhurst Clay (WDC)	558	498	0.3	Hopson *et al.* (2008)	Gallois and Worssam (1993)
Weald Clay (WC)	1671	1342	0.8	Hopson *et al.* (2008)	Gallois and Worssam (1993)

and is reflected by the shrinking and swelling of the ground. That is, the extent to which the soil shrinks as it dries out or swells when it gets wet.

The methodology for determining the VCP of the soils in this study was that determined by Jones and Terrington (2011) based on the modified plasticity index (I_P') proposed in Building Research Establishment (BRE) Digest 240 (BRE 1993*b*). The data were sourced from the BGS National Geotechnical Properties Database. At the time of this study, the national database contained data from more than 95 000 boreholes, comprising nearly 460 000 geotechnical samples, with more than 116 000 containing relevant plasticity data. The data validation and statistical evaluation processes were carried out in accordance with the methodology recommended by Jones and Terrington (2011) in order to quantify the I_P' of the soils

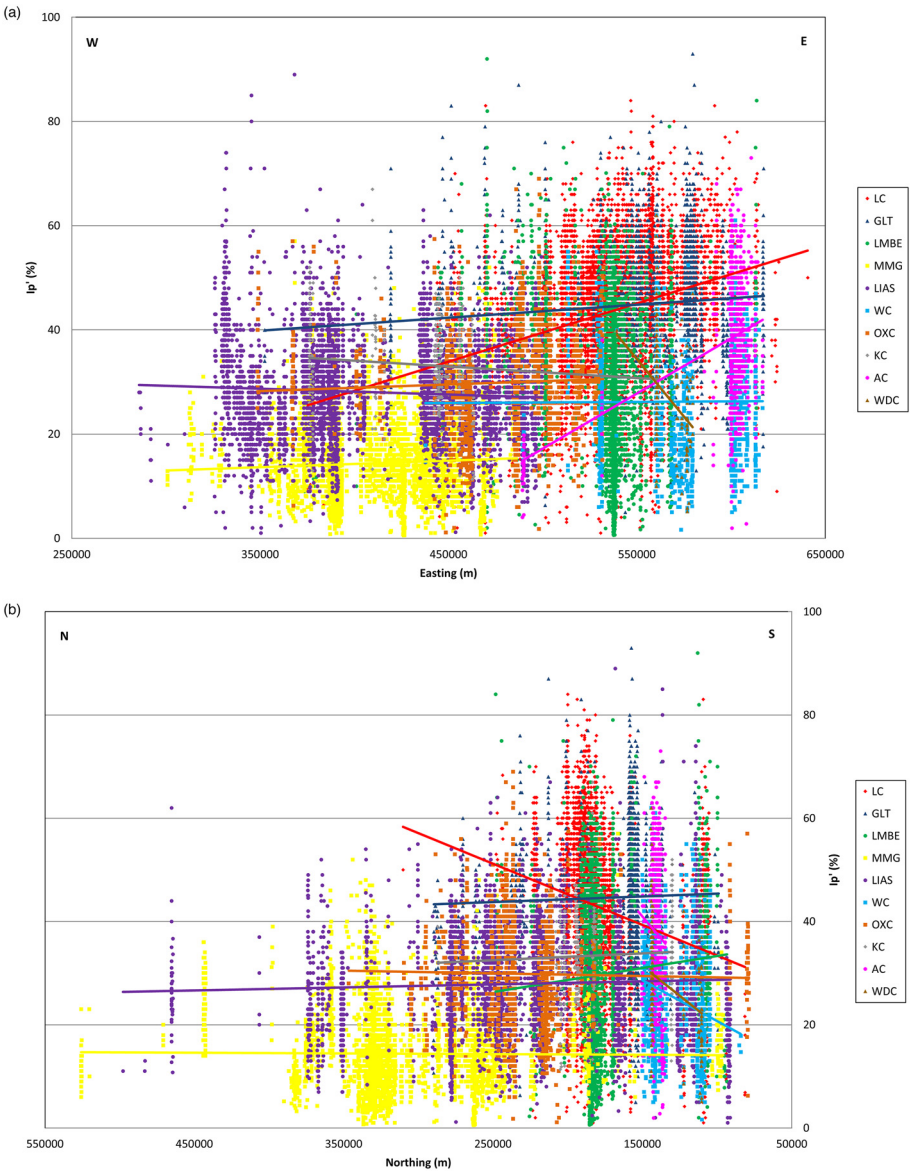

Fig. 2. Spread of data samples (whole outcrop) in (**a**) a west–east direction and (**b**) a north–south direction (see the text or Table 1 for the formation abbreviations).

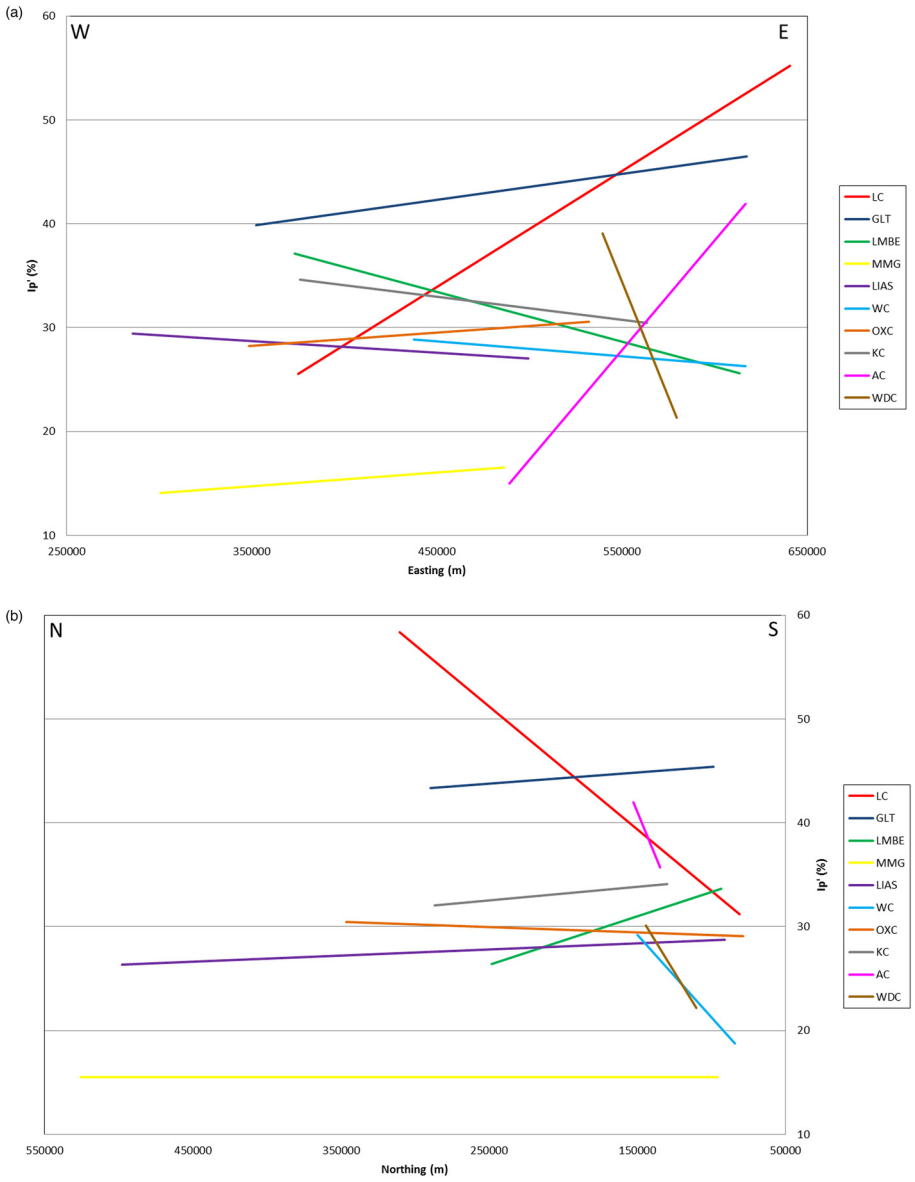

Fig. 3. Trend lines showing (**a**) a west–east direction and (b) a north–south direction (see the text or Table 1 for the formation abbreviations).

across their outcrops. After data validation, the number of 'acceptable' plasticity values used for the spatial interpretation was 41 575.

In order to try to quantify the VCP of all 10 formations a preliminary statistical evaluation of the I_P' values was carried out to determine the overall range of the data values with respect to their locations across the outcrop. This was carried out by plotting I_P' values against their Easting and Northing positions (Fig. 2a, b) to determine if any west–east, or north–south, trends of increasing plasticity were evident (Jones and Terrington 2011).

Table 2. Statistical analysis of I_P' (see the text or Table 1 for the formation abbreviations)

	LC	GLT	LMBE	MMG	LIAS	WC	OXC	KC	AC	WDC
Count	*13 149*	*2724*	*4565*	*4886*	*5929*	*1783*	*1284*	*306*	*811*	*207*
Minimum	1	5	1	1	1	2	1	11	2	5
0.005	10	14	2	1	7	6	6	12	7	6
0.025	19	23	7	4	12	9	12	16	14	10
0.1	29	33	14	8	18	13	18	24	23	17
0.25	37	39	20	10	22	19	23	28	30	22
Median	44	44	30	13	27	26	29	33	37	26
0.75	**50**	**51**	**38**	**17**	**33**	**33**	**36**	**39**	**48**	**34**
0.9	58	62	50	27	43	43	48	47	58	45
0.975	62	67	54	31	47	47	51	48	61	47
0.995	70	74	66	40	56	54	58	56	67	58
Maximum	84	93	92	57	89	62	69	67	73	62
Mean	43	45	30	14	28	26	30	33	38	28
Mode	45	46	30	13	28	29	26	31	30	26
VCP	**High**	**High**	Medium	**Low**	**Medium**	**Medium**	**Medium**	**Medium**	**High**	**Medium**

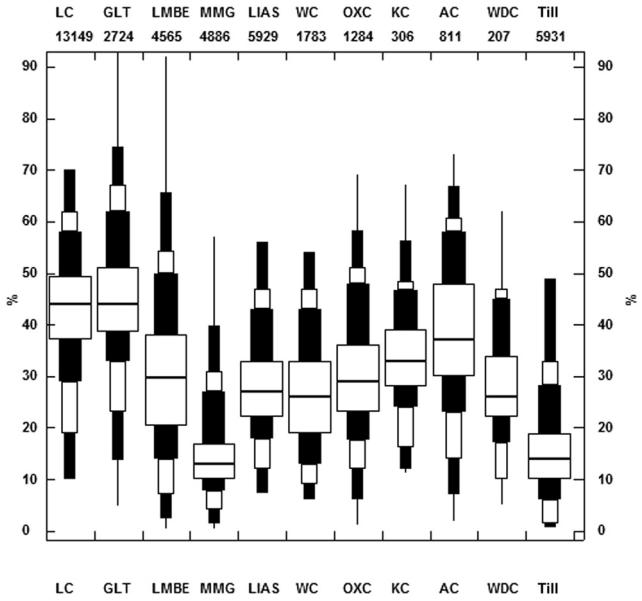

Fig. 4. Extended box and whisker plots of I_P' data values by formation (see the text or Table 1 for the formation abbreviations).

Table 3. Classification of VCP (BRE 1993a; Jones and Terrington 2011)

I_P' (%)	VCP
<10	Non-plastic
10–20	Low
20–40	Medium
40–60	High
>60	Very high

Figure 3a, b show the linear trend lines generated on the data, without the samples displayed. They show distinct directional trends of increasing plasticity for the formations:

- west–east and south–north: Atherfield Clay (AC), London Clay (LC) and Oxford Clay (OXC);
- west–east and north–south: Gault Clay (GLT);
- west–east only: Mercia Mudstone Group (MMG);
- east–west and south–north: Wadhurst Clay (WDC) and Weald Clay (WC); and
- east–west and north–south: Kimmeridge Clay (KC), Lambeth Group (LMBE) and Lias Clay (LIAS)

Summary statistics for these data across the 10 outcrops are presented in Table 2. These include a count of the number of I_P' data points for each formation, the minimum, maximum, mean, mode and median values, and a series of interquartile values, including the upper quartile and the lower quartile values. These statistics are illustrated in the form of extended box and whisker plots (Fig. 4). Extended box plots are constructed from the 0.5th, 2.5th, 10th, 25th, 50th, 75th, 90th, 97.5th and 99.5th percentiles of the datasets. The selected percentiles have been chosen as a compromise between practical geotechnics and statistical rigour (Hallam 1990; Jones and Terrington 2011).

Although, statistically, the median (50th percentile) value would normally be used as the most representative of shrink–swell behaviour, it was decided that in order to portray the 'worst-case' scenario, and represent a greater proportion of the data, the procedure determined by Jones and Terrington (2011) that utilizes the upper quartile (75th percentile) value would be used in this study.

The VCP was calculated from the statistically analysed I_P' data and a classification made based on the upper quartile values. The I_P' values for the 41 575 data points were each allocated a classification ranging from non-plastic to very high; these subdivisions are shown in Table 3 and the percentage VCP, by classification, are summarized in Table 4.

Table 2 shows that the GLT and the LC both have upper quartile values of I_P' of ≥50%, and the AC has a value of 48%, giving them all a VCP of high. However, Figure 4 and Table 4 show that 71% of the GLT samples and 67% of the LC samples fall in the high–very high classification range, and 90% of the AC samples fall in the medium–high range.

Table 2 shows that the KC, the OXC and the LMBE have upper quartile values of I_P' of 35–40%, giving them all a VCP of medium. However, Figure 4 and Table 4 show that 95% of the KC samples and 85% of the OXC samples fall in the medium–high classification range, and 95% of the LMBE samples fall in the low–high range.

Table 2 shows that the LIAS, WDC and WC have upper quartile values of I_P' of 30–35%, giving them all a VCP of medium. However, Figure 4 and Table 4 show that 76% of the LIAS samples and 75% of the WDC samples fall in the medium classification range, and 89% of the WC samples fall in the low–medium range.

Table 2 shows that the MMG has an upper quartile value of I_P' of 17%, giving it a VCP of low. Figure 4 and Table 4 back this up, showing that 63% of the MMG samples fall in the low classification range.

Plots of I_P' values against depth for the 10 formations are presented in Figure 5a (AC, LC and OXC), b (GLT and MMG), c (WC and WDC) and d (KC, LIAS and LMBE). They are grouped in this way because of their similar east–west, north–south trends, and to make the data easier to see. These profiles show the sample data based on their depth below ground level.

The profiles in Figure 5a show that, for AC, 90% of the data lie in the medium–high VCP classification range (I_P' = 23–58%), with a slight decrease in plasticity with depth. For LC, 67% of the data lie in the high–very high VCP classification range (I_P' = 44–70%), with a trend of increasing plasticity with depth. For the OXC, 85% of the data lie in the medium–high VCP classification range (I_P' = 23–58%), with a slight decrease in plasticity with depth.

The profiles in Figure 5b show that, for the GLT, 71% of the data lie in the high–very high VCP classification range (I_P' = 44–74%), with a minimal change in plasticity with depth. For the MMG, 63%

Table 4. Range and amount of VCP calculated by formation (see the text or Table 1 for the formation abbreviations)

VCP	Percentage of samples by classification									
	LC	GLT	LMBE	MMG	LIAS	WC	OXC	KC	AC	WDC
Non-plastic			4	19	1	3	1		1	2
Low	2	1	18	63	14	25	14	5	5	13
Medium	31	28	56	17	76	64	68	73	50	75
High	63	63	21	1	9	8	17	22	40	10
Very high	4	8	1					1	3	

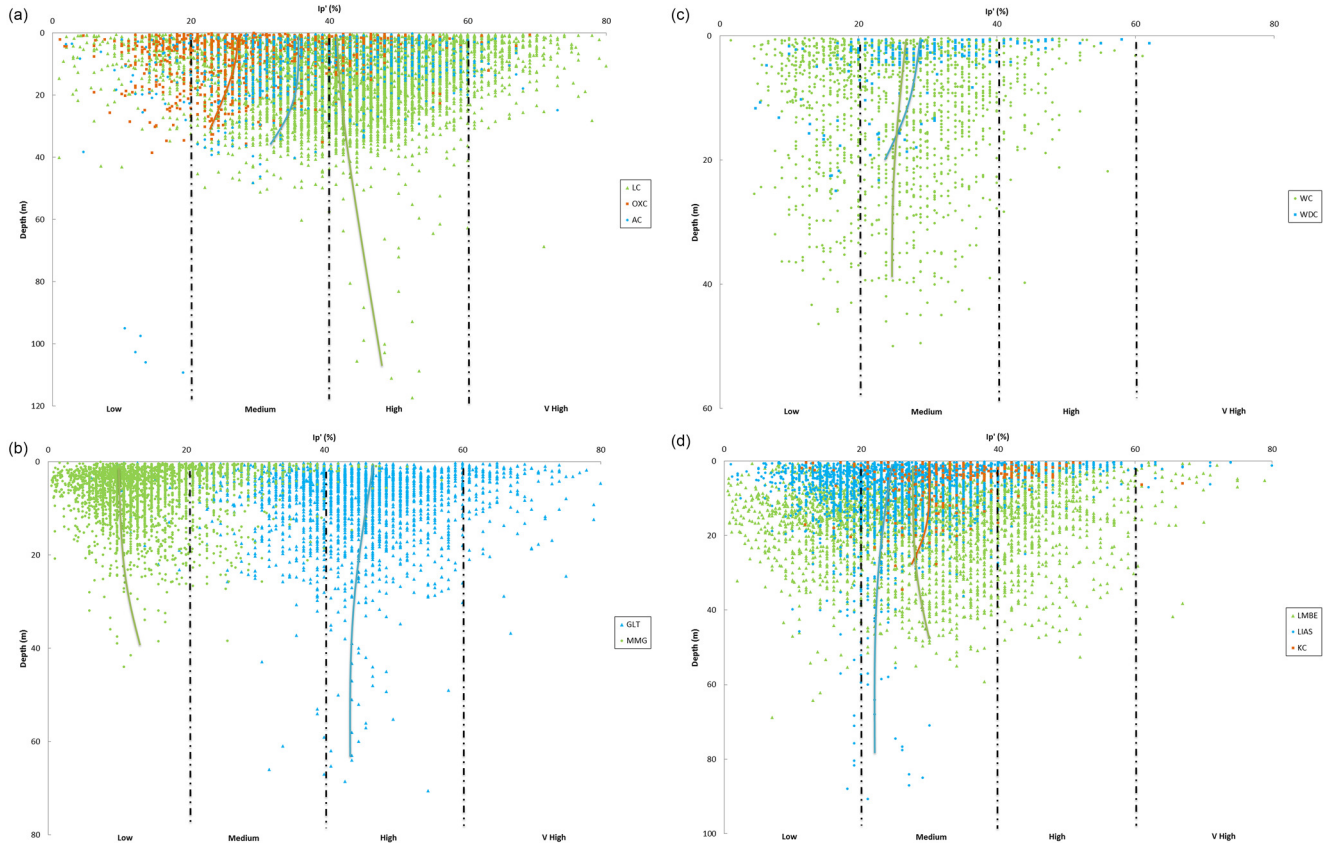

Fig. 5. (**a**)–(**d**) I_P' v. depth profiles (by formation; see the text or Table 1 for the formation abbreviations).

of the data lie in the low VCP classification range ($I_P' = 10$–17%), with a slight increase in plasticity with depth.

The profiles in Figure 5c show that, for the WC, 89% of the data lie in the low–medium VCP classification range ($I_P' = 13$–33%), with a minimal change in plasticity with depth. For the WDC, 75% of the data lie in the medium VCP classification range ($I_P' = 22$–34%), with a slight decrease in plasticity with depth.

The profiles in Figure 5d show that, for the KC, 95% of the data lie in the medium–high VCP classification range ($I_P' = 24$–39%), with a slight decrease in plasticity with depth. For the LIAS, 76% of the data lie in the medium VCP classification range ($I_P' = 22$–33%), with a minimal change in plasticity with depth. For the LMBE, 95% of the data lie in the low–high VCP classification range ($I_P' = 14$–54%), with a slight decrease in plasticity with depth.

However, with large amounts of data, covering such wide areas, it is difficult to determine the changes in plasticity to any great detail. Therefore, another method of examining the data, such as 3D modelling, is required.

Spatial interpretation

As shown above, variations in plasticity with area and with depth can be depicted using purely statistical methods. However, the profiles show that these methods do not reveal the true multi-dimensional variations of the formation. To do this a more suitable method of modelling the data, such as 3D interpolation, is required.

Interpolation estimates values at unknown locations based on known samples (Lam 1983). The inverse distance weighting (IDW) interpolative technique described by Jones and Terrington (2011) was applied to the data for all 10 formations in order to determine whether any spatial trend in plasticity was evident. IDW (in this instance) is the estimation of the VCP value at any given location determined by a weighted mean of the nearby values. This output value is limited to the range of the values being used to interpolate it, and therefore the average can never be higher than the greatest value or less than the lowest value. The IDW technique was applied to the dataset using the geostatistical analysis extension in the Esri ArcMap 10 geographical information system (GIS).

To identify whether any directional trend existed in the I_P' values for all 10 formations, the outcrop were analysed, observing all available sample points and ignoring variations with depth. However sizable gaps in the distribution of samples across the outcrop are likely to have influenced the interpolation model. The resulting spatial analysis using the IDW interpolative technique showed that, although there are localized exceptions, possibly as a result of the 'bulls-eye' effect, the VCP tends to increase in a west–east direction (Fig. 6), with no south–north trend. However, Figure 3a shows that only AC, LC, OXC, GLT and MMG have a west–east trend, and Figure 3b shows a definite south–north trend for AC, LC, OXC, WDC and WC.

Jones and Terrington (2011) discussed the issues of generating plots based on geographically sparse data at different depth intervals down a borehole. They concluded that both the sparsity of data and depth have an effect on the interpolation carried out. To generate a statistically defined model, an area with a large amount of well-spaced data within a specified and statistically influential distance from known sample locations and at variable depth is required. 'Splitting' the data out to its component formations was also deemed necessary.

3D modelling

To construct a more representative model of spatial VCP variations in clay-rich formations, utilization of a more sophisticated 3D modelling and visualization package is necessary. The NextMap Digital Terrain Model (DTM: Intermap Technologies) was used to constrain the data at the ground surface, including the boreholes, and as the top constraining surface for the voxel models. The original

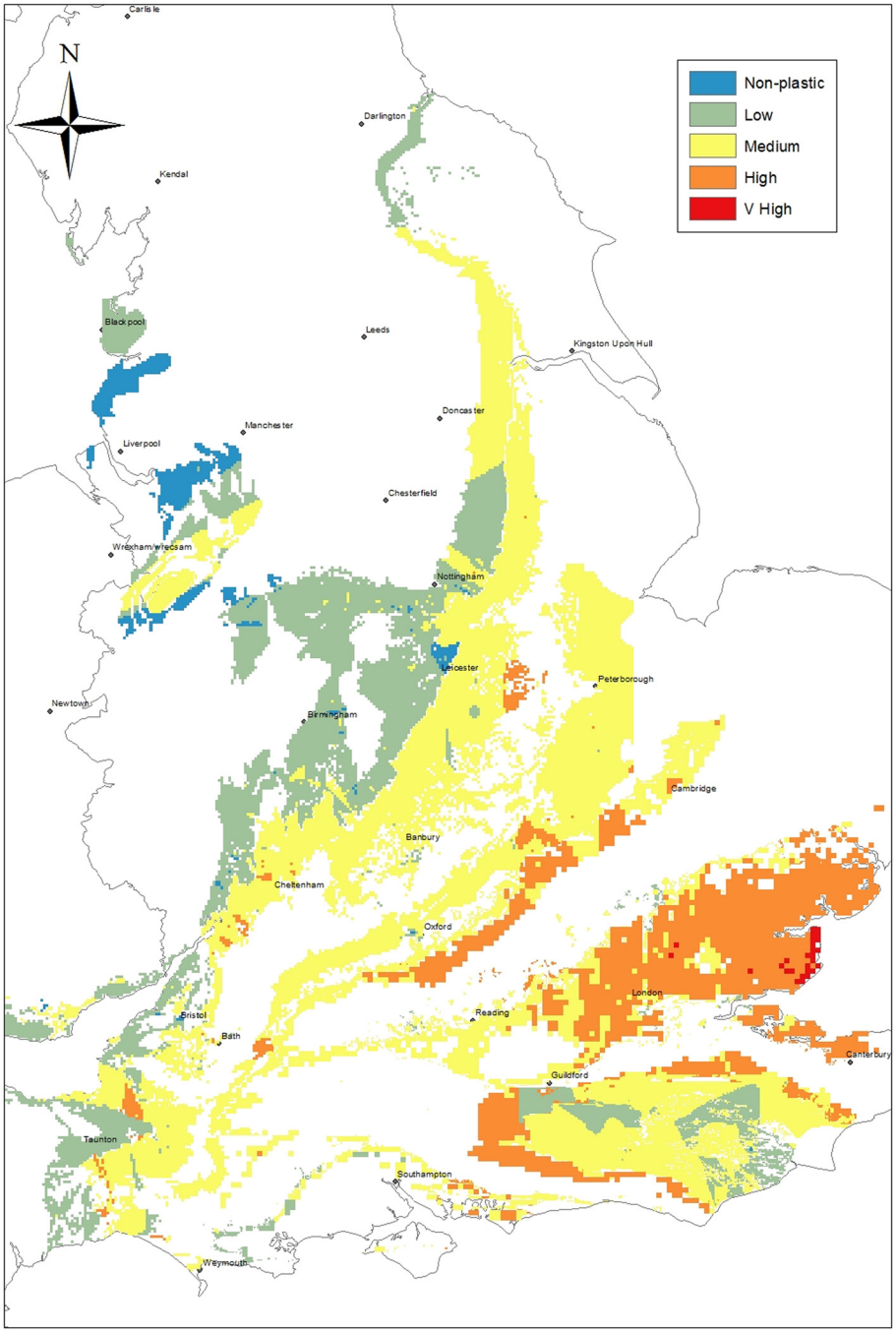

Fig. 6. IDW interpolation for all formations using mean I_P' at each sample location.

data had a 5 m cell resolution. The data were subsampled to a lower resolution (100 m) to ensure that the entire dataset could be modelled in the area of interest. The borehole and surface sample information were then 'hung' from the DTM to give it an accurate position below ground level. To visualize the data as accurately as possible, it was decided to create an S-Grid model; a flexible 3D grid that can be eroded between two boundary horizons to model a volume: for example, the ground surface (DTM) and the base of the LC. Culshaw (2005) gave an example of this approach using SPT 'N' value data for glacial till in the Manchester/Salford (UK) area. This paper follows the approach used by Jones and Terrington (2011) to create their 3D VCP model. S-Grid models can also contain multiple property information, and fit the boundaries of the data more accurately.

S-Grid models were created using the '3D grid reservoir builder' in GoCAD^{TM}, with the DTM set as the upper limit, the DTM −30 m surface as the basal limit and the outcrop of each formation as the area boundary. The modified I_P' values were draped onto the S-Grid to 'paint' the grid cells (each cell containing an I_P' value was transformed to that I_P' value). The grid was then initialized to the mean value (derived by the builder), giving all cells without a 'painted' I_P' value the mean value. The modified I_P' values were then interpolated and smoothed throughout the grid, giving a full 3D image. S-Grids provide a seamless interpolation of the modified I_P' data, showing a visualization that allows the I_P' values to be examined relative to ground level, as opposed to just seeing the trends within the data themselves. Visualizing the data with the DTM gives a greater sense of reality and perspective. IDW allows only snapshots at different depth intervals but the S-Grid allows interactive and dynamic visualizations of the data at various depths and locations. Combining these GIS and 3D modelling capabilities, a prediction of plasticity and, hence, the VCP becomes a realistic prospect.

Looking at the central and eastern area of the LC (from Jones and Terrington 2011) the IDW model shows little variation in plasticity in the uppermost part of the LC, which falls mainly within the high

VCP class (Fig. 7a). However, as the depth increases to 8 m or more, an area of increased plasticity equating to a very high VCP classification can be seen in the east of the area (Fig. 7b). At a depth of *c*. 20 m, the VCP in the east remains very high, decreasing to medium VCP in the west (Fig. 7c). This trend continues to a depth of *c*. 30 m (Fig. 7d).

Facies modelling techniques have been used widely at the BGS to convey lithological variation and heterogeneity of geotechnical parameters (Kearsey *et al.* 2011, 2015; Woods *et al.* 2015), and are a standard geological modelling output for other modern geological surveys, such as The Netherlands Organization for Applied Scientific Research (TNO) (Stafleu *et al.* 2012). Facies models can be used to produce multiple realizations of the variation of parameters such as the lithology (e.g. the proportion and grading of sand, gravel, silt and clay) across a domain where there is an abundance of *XYZ* data from boreholes or point samples. Instead of a sharp boundary depicting the classification of what becomes a stratigraphic horizon, as typically shown in geological maps and deterministic models (Kessler *et al.* 2009), facies modelling allows these lithologies to grade into each other, which better captures the interfingered nature of heterolithical geological deposits and their associated physical properties.

Previous attempts to map and model the VCP of the LC in central London (Jones and Terrington 2011) using basic facies techniques showed that the modified plasticity values (I_P') used to generate the VCP score ranged from 1 to 80+ and also varied significantly in their *XYZ* position. The variation in values and the clustered and sometimes linear alignment of the data (coming from road or railway developments) can obscure the visualization of relationships between the data. Often the *XY* scale was set at 100 × 100 m, or coarser, but the *Z* scale tended to be 1–2 m as the sampling rate downhole is sub-metre. Therefore, the more traditional facies techniques for modelling this type of continuous data, such as IDW, are limited in areas where there are large gaps between the data points and the data are clustered, as the I_P' values are interpolated beyond what is reasonably expected, thus masking the accuracy and uncertainty in areas where there are few data points.

To gain a better understanding of the variations within the dataset, the I_P' values were grouped into the classifications outlined in Table 3. These data were used discretely to produce facies models based on the classifications. The methodology used follows that by Jones *et al.* (2017) in SKUA-GOCAD™. The detail and benefits of this methodology are described by Kearsey *et al.* (2015), although there are some fundamental differences between that methodology and the one used in this study, with the main one being that physical geotechnical parameters were assessed here – namely I_P' and VCP – rather than just the lithological variation assessed in Kearsey *et al.* (2015).

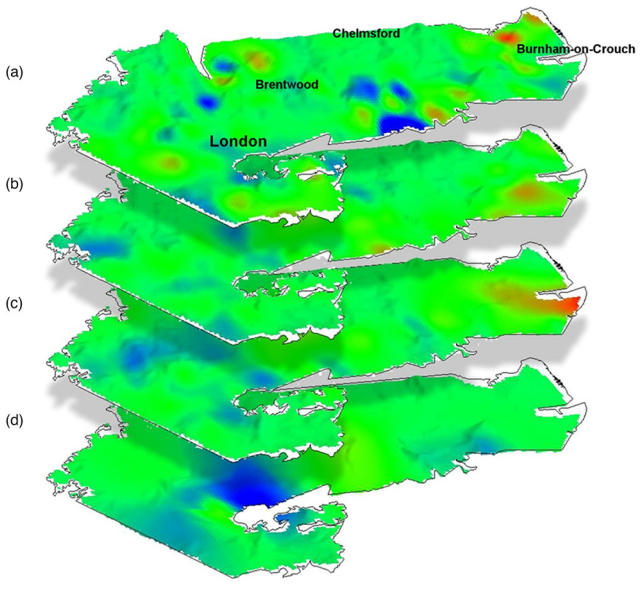

Fig. 7. S-Grid interpolations for London Clay, showing surfaces at (**a**) 0, (**b**) 8, (**c**) 20 and (**d**) 30 m (blue, medium VCP; green, high VCP; yellow/red, very high VCP).

The models created using this technique should show a better reflection of the true nature of the ground conditions relating to the VCP of the clay units. However, these models do not generate good site-specific results and do not capture locally constrained variations, but rather give an overall impression of the shrink–swell properties of that specific clay unit. More detailed site-scale models can be produced for areas where large numbers of boreholes and sample data are situated and evenly distributed.

S-Grid models were created for each of the clipped formation areas and then cross-sections were extracted in order to show the full 3D potential of the technique used. Figure 8 shows the extent of the clipped area of the LC and the VCP values visible at the surface of the formation. The model shows little variation in the plasticity across this area, in the surface of the London Clay, falling mostly within the high VCP class, as it showed with the previously discussed IDW model and the simpler S-Grid model.

Figure 9 shows the base of the London Clay for the extent of the clipped area, with the I_P' sample points displayed with their VCP value, and the lines of the four digitized cross-sections marked. The sections were chosen because they represented areas with large amounts of well-spaced data, usually aligned to a linear feature (such as a road). The digitized cross-section number 1 (Fig. 10) confirms the west–east trend of increasing plasticity, whilst also showing that the London Clay, in this area, maintains a high VCP value throughout its depth. S-grid models and cross-sections were also created for the AC, GLT, LIAS, LMBE and MMG, as discussed below. S-grid models were not created for the KC, WDC and WC formations because the data were too sparsely distributed and the interpolation was deemed to not be good enough.

Figures 11–15 show a single digitized cross-section from each of the other five clipped formation areas, these being the AC, GLT, LIAS, LMBE and the MMG. Interpretations of these figures indicate that the AC (Fig. 11) shows a slight increase in plasticity in a west–east direction, comparing well with Figure 3a, and an increase with depth in the east. The shape of the lower boundary is disconformable on the WDC throughout the Wessex Basin, on the Vectis Formation in the Vectian Basin, and on the WC in the Wealden Basin. The GLT (Fig. 12) also shows a west–east trend of increasing plasticity. This compares well with the results obtained from Figure 3a, which shows the same west–east trend of increasing plasticity. It also shows that the GLT increases in plasticity with depth across the section.

The cross-section of the LIAS (Fig. 13) shows that it maintains a medium VCP across the section, with no discernible east–west, north–south or depth trend. This compares well with Figure 3a, which showed only minor trends. The LMBE (Fig. 14) also maintains a medium VCP across the section. This does not compare well with the results from Figure 3a, which showed slight east–west and north–south trends of increasing plasticity. However, this could be due to the orientation of the sections chosen, or perhaps the lack of data in *XY* or at depth.

Figure 15 shows a west–east cross-section of the MMG and confirms the results from Figure 3a that there is no discernible trend in increasing plasticity in either an east–west or north–south direction. The section shows that it maintains a low VCP throughout, including throughout its depth.

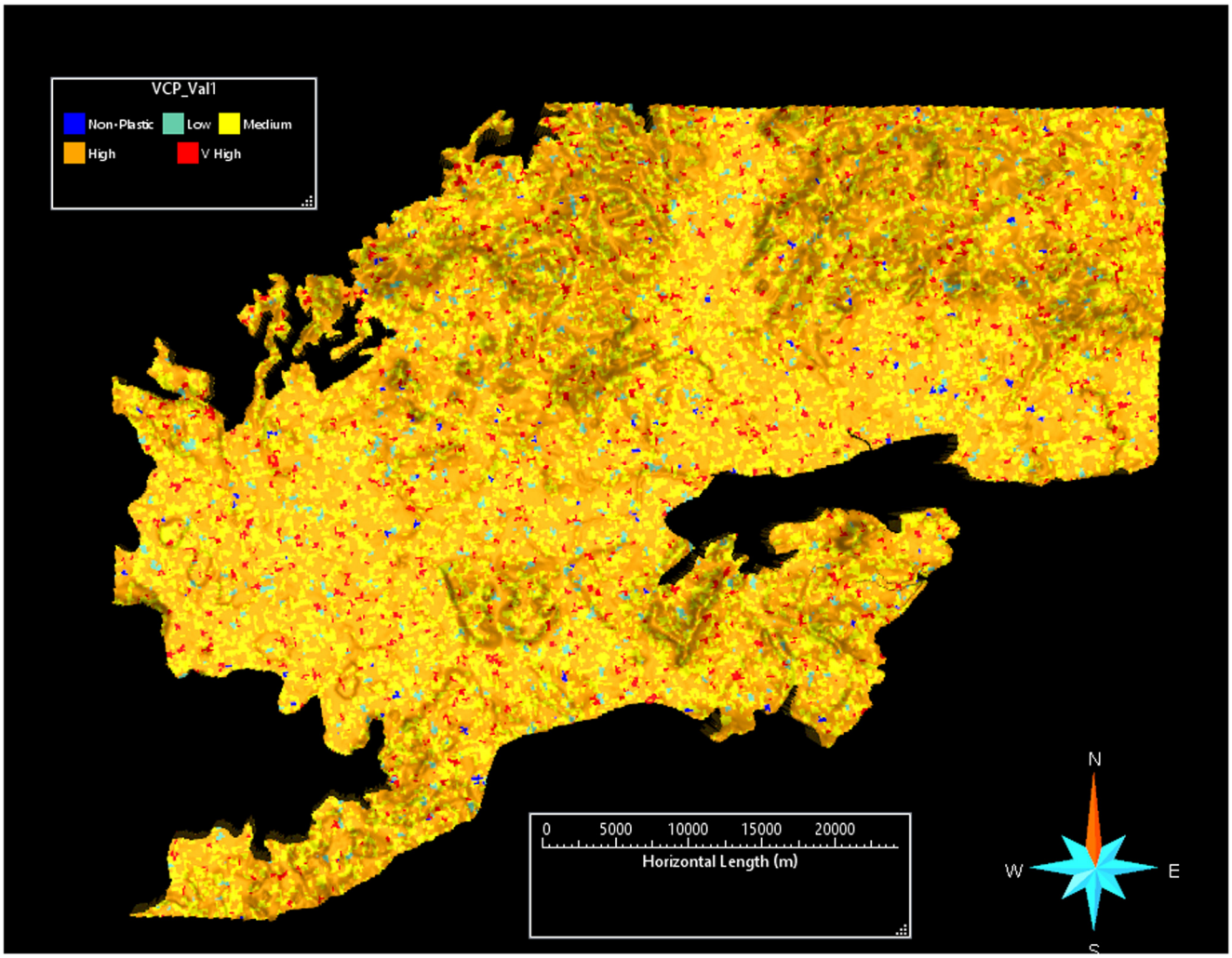

Fig. 8. S-Grid model of the clipped area of London Clay (LC), showing the top surface.

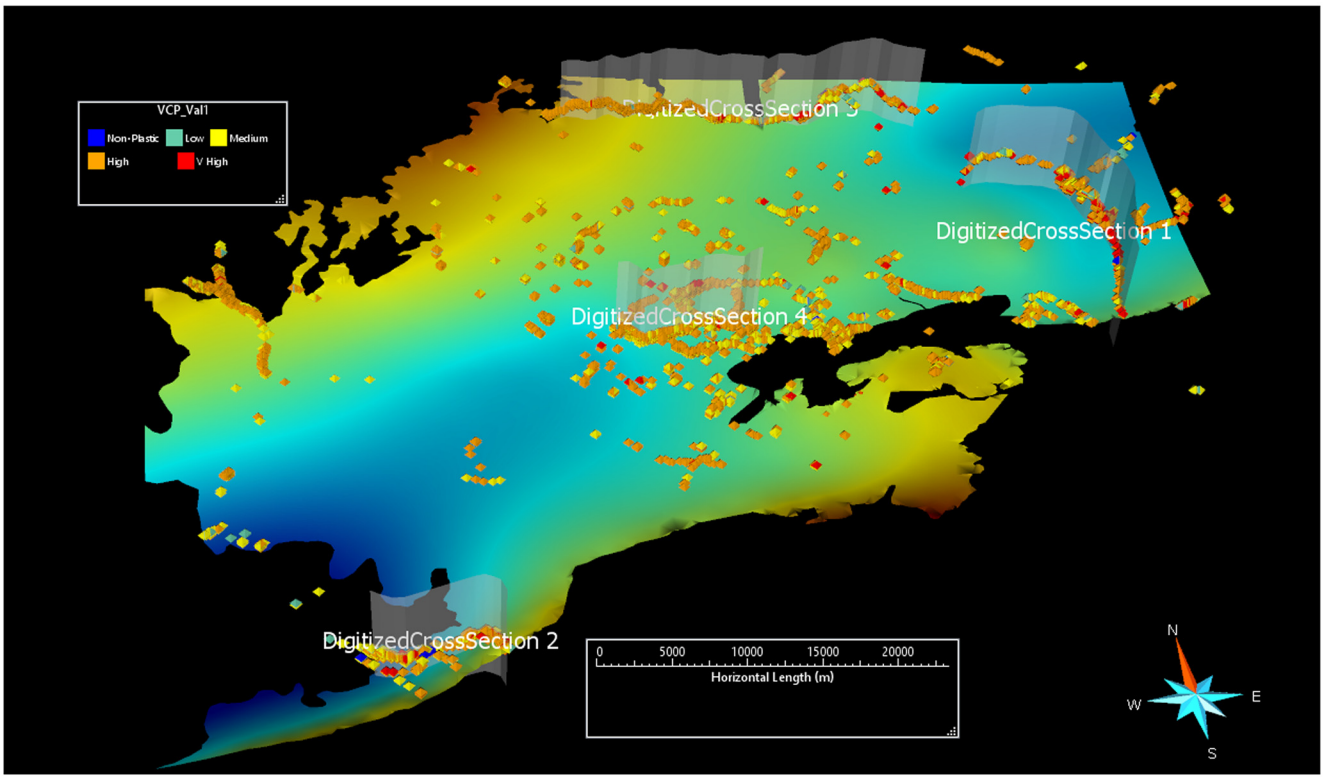

Fig. 9. S-Grid model of the clipped area of London Clay (LC), showing areas of digitized cross-sections.

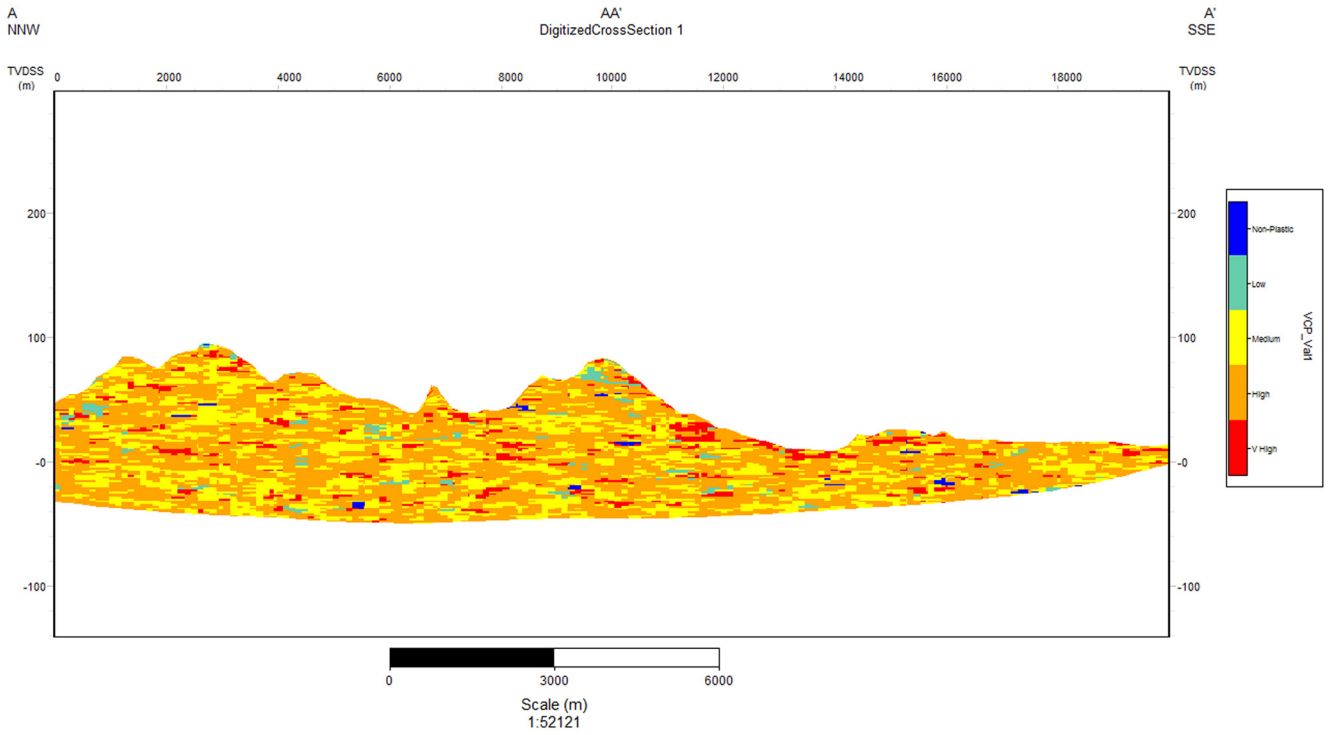

Fig. 10. Digitized cross-section 1 of London Clay (LC), showing VCP values. TVDSS, true vertical depth subsea.

GeoVisionary is the result of a lengthy collaboration between the BGS and Virtalis Ltd. It is a unique 3D stereographic software system that allows the high-resolution visualization and interpretation of geospatial data, used for mapping and data interrogation, from continent to site-specific scales (Terrington *et al.* 2015). GeoVisionary also allows the integration of 3D and 4D data, such as 3D geological model data including boreholes (both vertical and deviated), cross-sections and surfaces, as well as parameterized voxel models, LiDAR point cloud scans, CAD models of buildings and infrastructure, and time-series data that could show land-level change or water-table variation, for example.

The clipped area of the LC was re-cropped to form a smaller area (Fig. 16) centred around Islington, where there was a large data density of I_P' values, making it easier to import into GeoVisionary as a voxel model. The model can be displayed with other geospatial data (e.g. the outcrop and underlying geology: Fig. 17) or it can be clipped to show a plane of VCP through any section of the model (Fig. 18). GeoVisionary can also show either multiple or singular

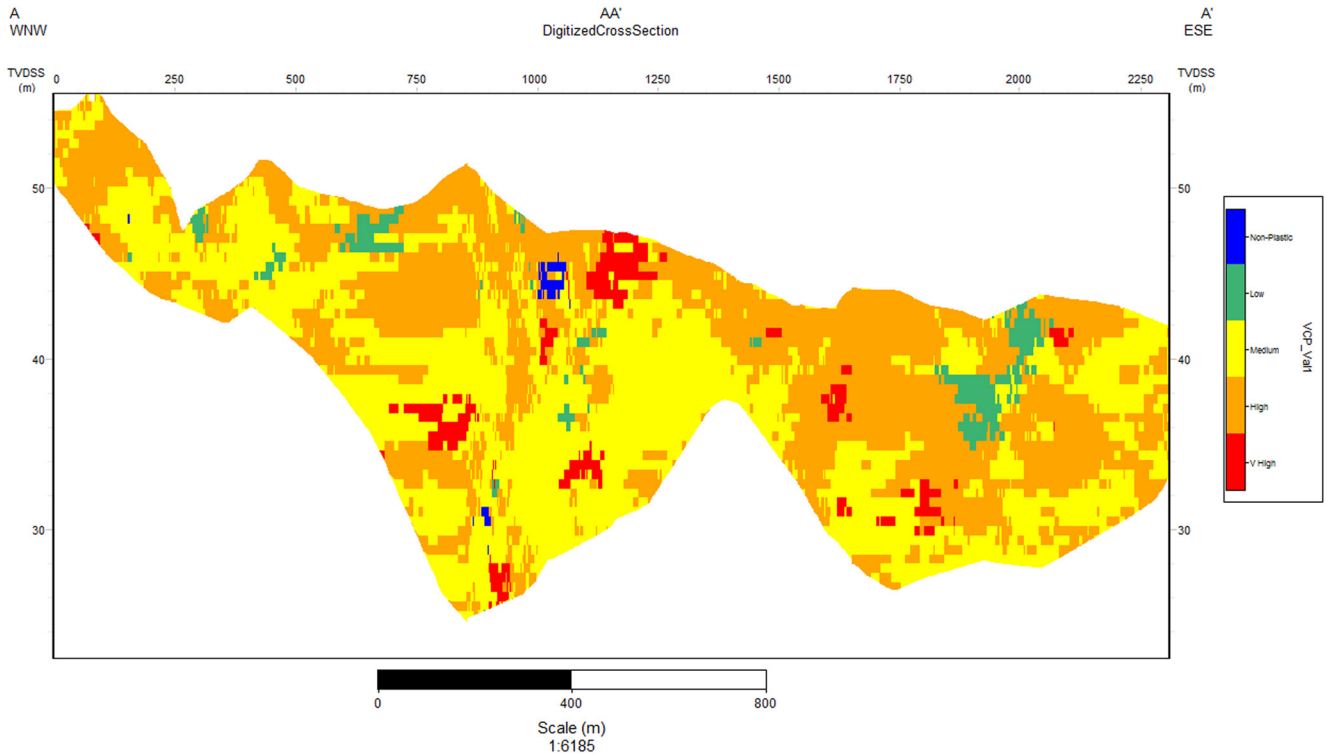

Fig. 11. Digitized cross-section 1 of Atherfield Clay (AC), showing VCP values. TVDSS, true vertical depth subsea.

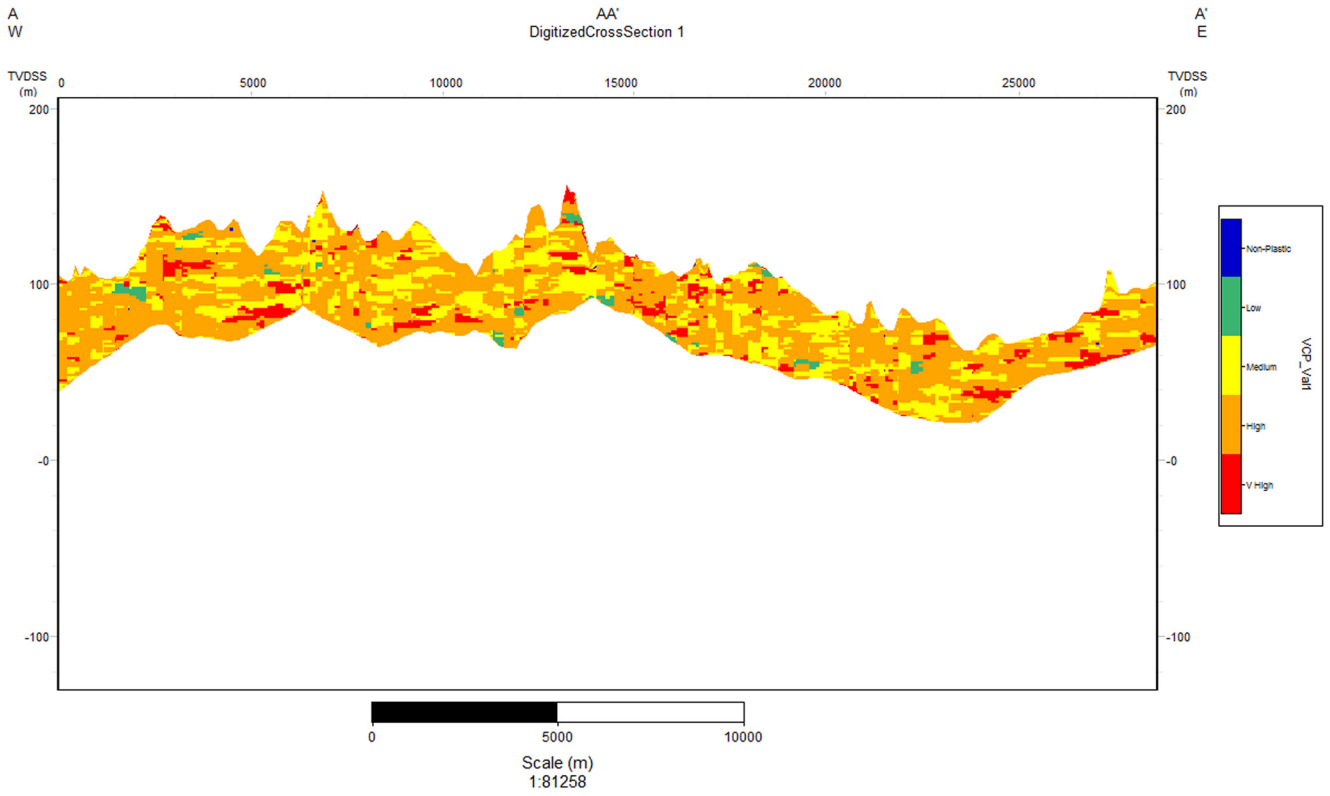

Fig. 12. Digitized cross-section 1 of Gault Clay (GLT), showing VCP values. TVDSS, true vertical depth subsea.

values of VCP; Figure 19, for instance, shows the re-cropped area displaying only the very high VCP values.

The BGS GeoSure dataset comprises six different GIS 1:50 000-scale layers, with each layer representing a different natural ground stability hazard that occurs in Great Britain (Walsby 2008): (1) collapsible ground; (2) running sands; (3) compressible ground; (4) landslides; (5) soluble rocks; and (6) shrink–swell (Fig. 20). The current version of the GeoSure dataset is v. 9.0 and this was released in 2024. The GeoSure datasets are 2D polygon (area) layers resulting from deterministic assessments of appropriate causative factors. Each

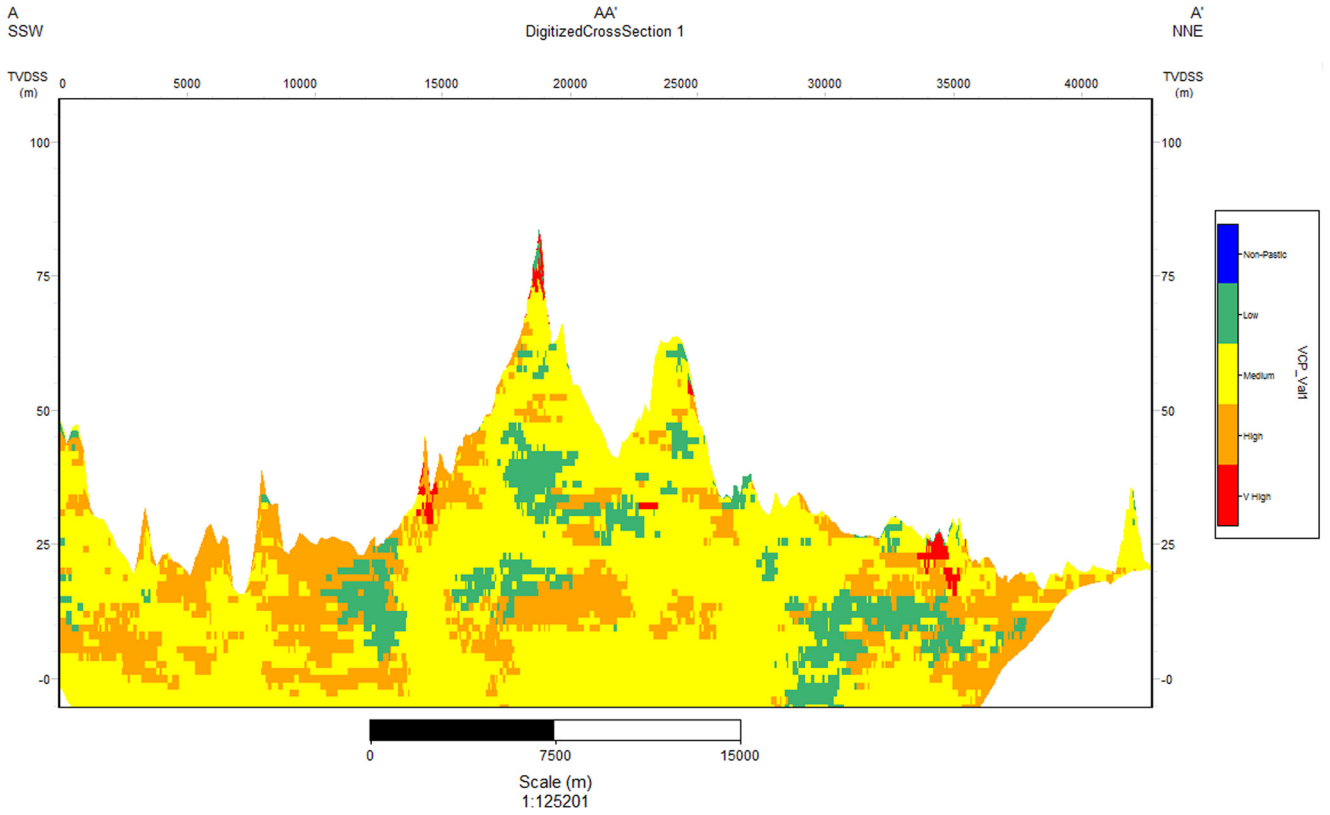

Fig. 13. Digitized cross-section 1 of Lias Clay (LIAS), showing VCP values. TVDSS, true vertical depth subsea.

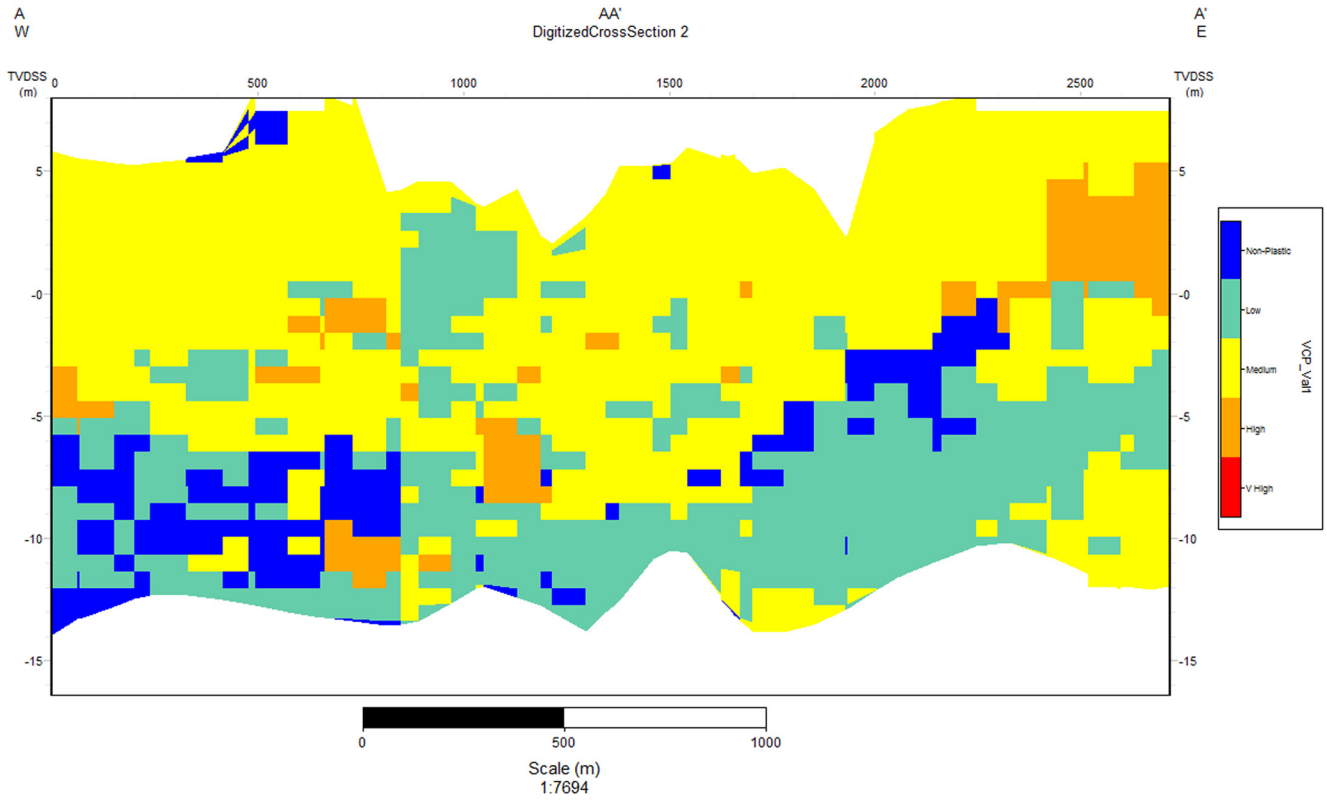

Fig. 14. Digitized cross-section 1 of the Lambeth Group (LMBE), showing VCP values. TVDSS, true vertical depth subsea.

ground stability geohazard is classified using the same straightforward classification, ranging from 'A' (low hazard potential) to 'E' (high hazard potential). The GeoSure shrink–swell layer was used to determine the VCP values for the clay soils herein. Figure 20 shows the shrinkage potential of all the lithologies across the UK mainland as moderate or significant. This potential can be shown at greater resolution but is lost on such a small-scale map.

The GeoSure shrink–swell 3D dataset, produced in 2023, is an addition to the GeoSure ground-stability data that consists of a single data layer, in GIS format, which identifies areas of potential

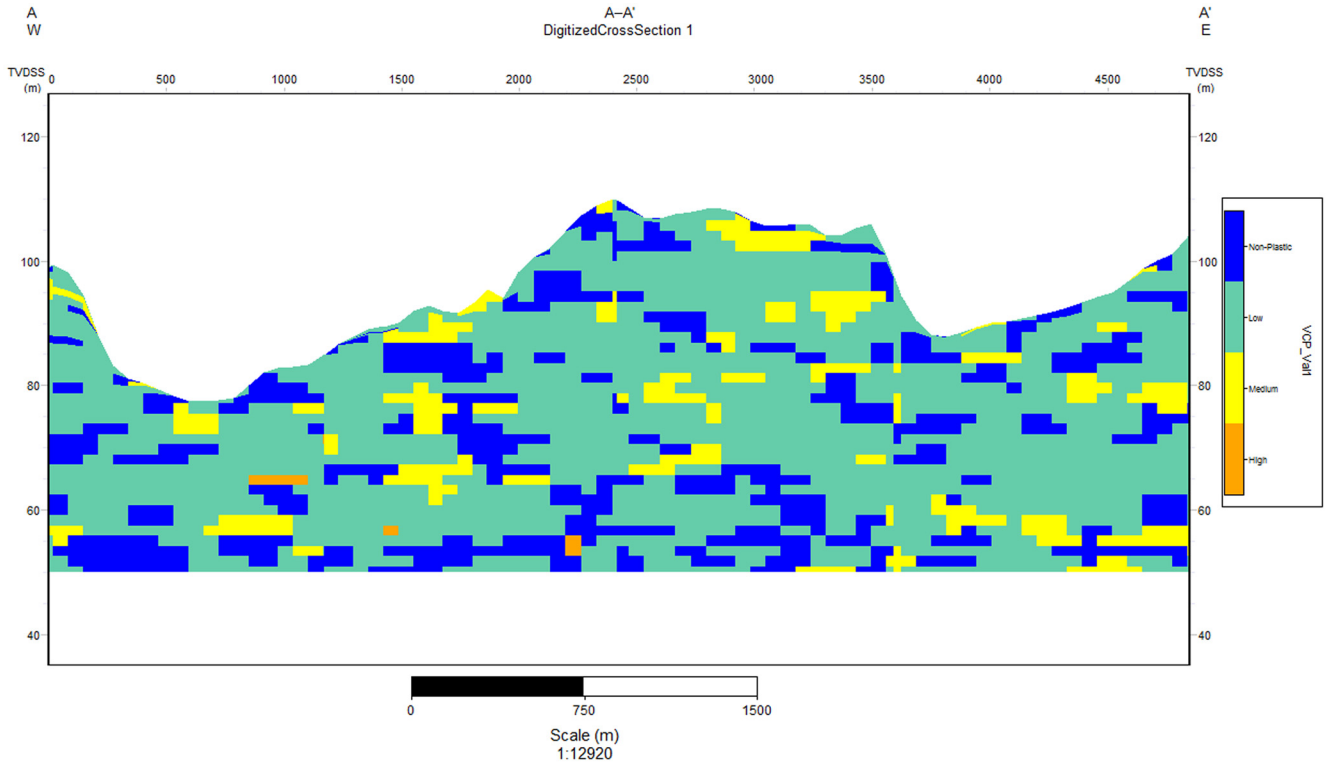

Fig. 15. Digitized cross-section 1 of the Mercia Mudstone Group (MMG), showing VCP values. TVDSS, true vertical depth subsea.

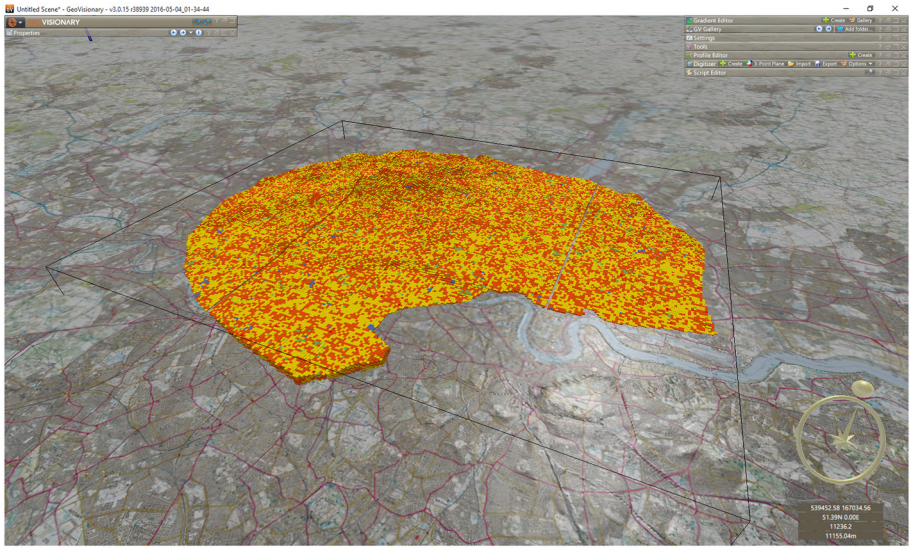

Fig. 16. GeoVisionary image of the S-Grid model of the re-cropped area of London Clay, showing VCP values overlaid on the map.

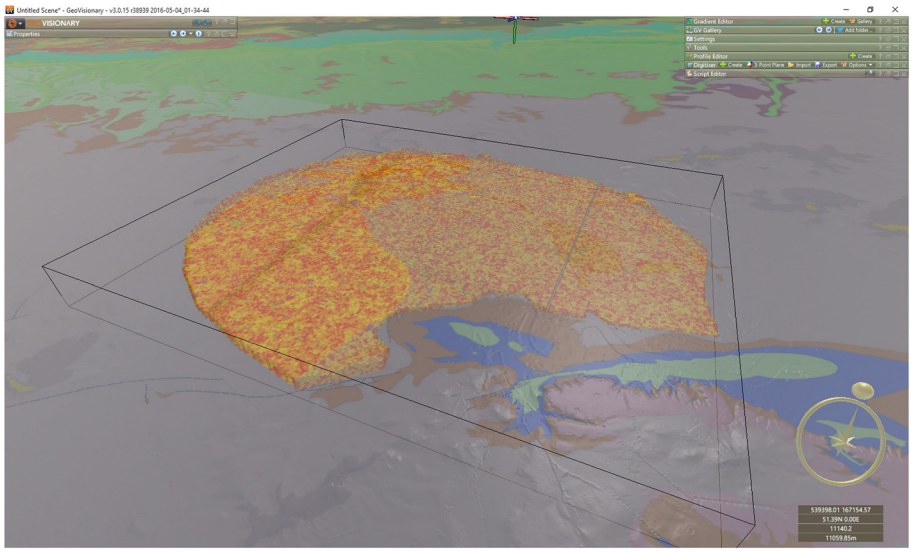

Fig. 17. GeoVisionary image of the S-Grid model of the re-cropped area of London Clay, showing the outcrop and underlying geology.

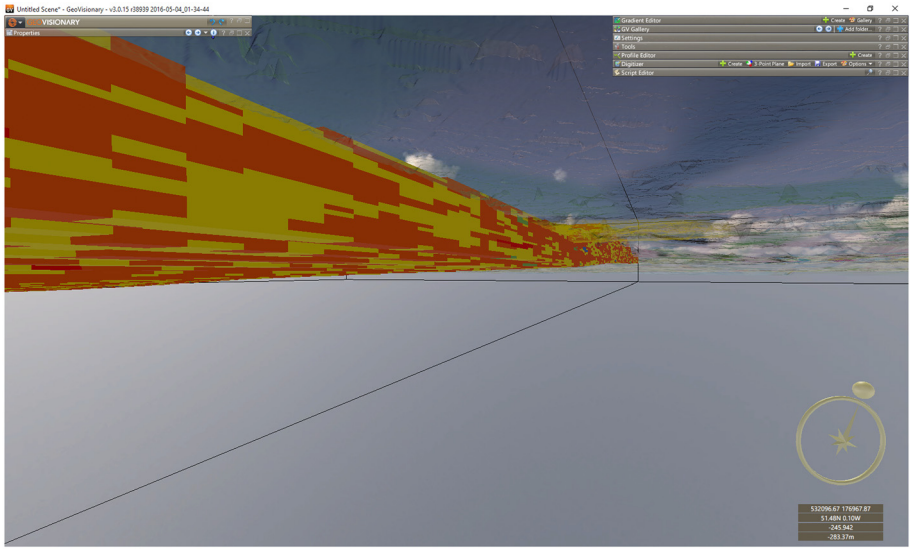

Fig. 18. GeoVisionary image of the S-Grid model of the re-cropped area of London Clay, showing VCP values as a clipping plane.

shrink–swell hazard, in 3D space, at intervals down to 20 m in the London Lithoframe (Mathers *et al.* 2014) area of Great Britain.

The BGS London Lithoframe geological model (Mathers *et al.* 2014) covers an area extending 120 km east–west and 40 km north–south (4800 km^2). The model was constructed as 12 squares (20 × 20 km) arranged as six columns in the east–west direction and two rows in the north–south direction (Fig. 21). The GeoSure Shrink–Swell 3D model uses the 12 subareas defined by the London

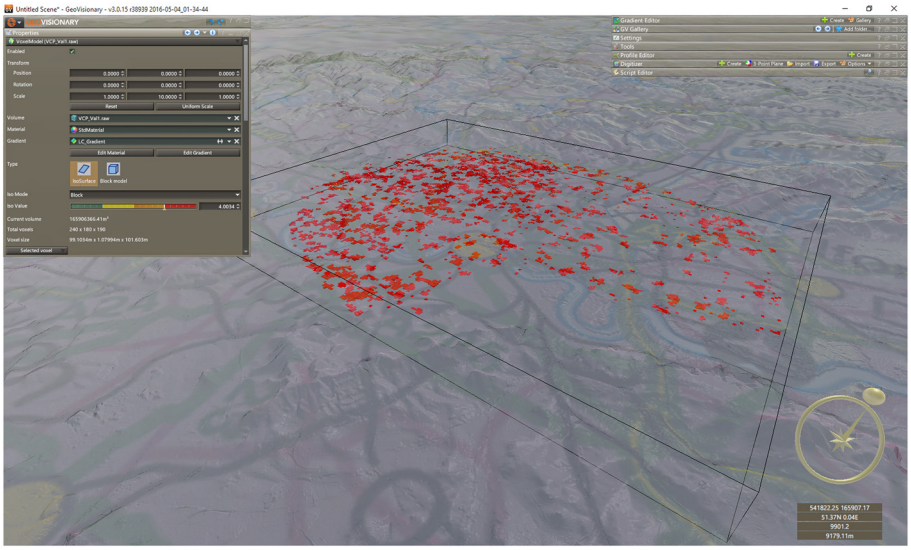

Fig. 19. GeoVisionary image of the S-Grid model of the re-cropped area of London Clay, showing 'very high' VCP values.

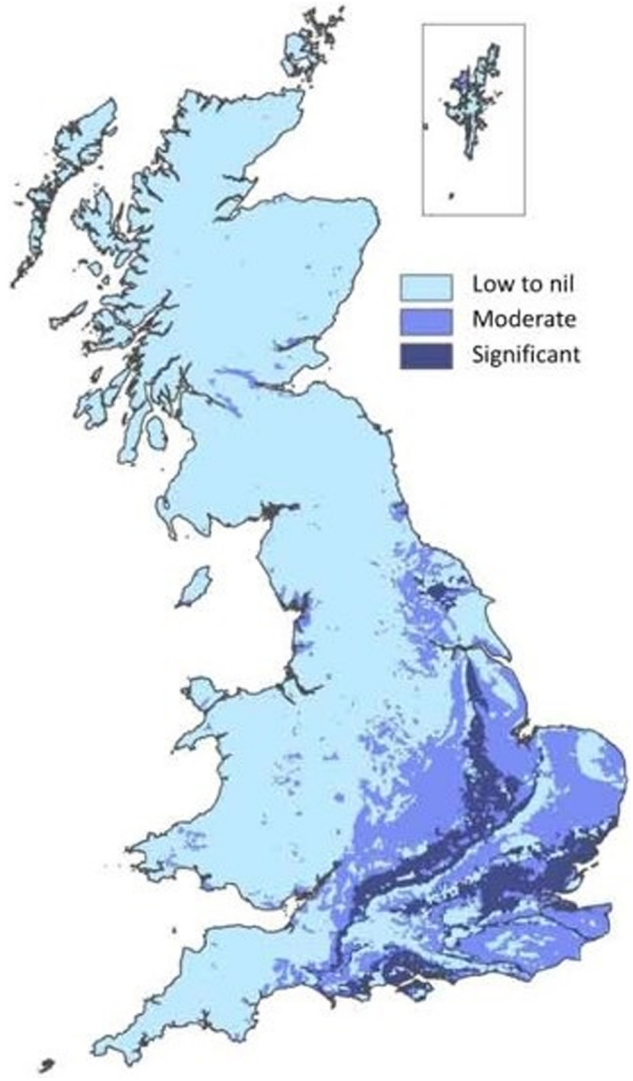

Fig. 20. UK map of the GeoSure shrink–swell geohazard. Source: Lee and Diaz (2017), https://www.bgs.ac.uk/datasets/bgs-geosure-shrink-swell-subsurface/; contains Ordnance Survey data © Crown Copyright and database rights 2020.

Lithoframe model, and within them it contains the shrink–swell characteristics of the top 20 m of the LC.

Esri ArcGIS software was used to create the GeoSure Shrink–Swell 3D model. The model area was defined by a regular 50 × 50 m grid, then converted to a point feature class, with each point located at the centre of a grid cell. The Nextmap DTM (Intermap Technologies 2007) defined the ground elevation (related to Ordnance Datum) of each point. A custom Python script assessed the presence below each point of geological formations at nine specific depths (at 0, 1, 2, 3, 4, 5, 6, 7, 8, 9, 10, 15 and 20 m) and stored this information as an attribute-string attached to each point. A second custom python script converted this attributed point dataset to a series of nine gridded surfaces with 50 × 50 m resolution, each defining the geological conditions at the specified depth.

The GeoSure Shrink–Swell 3D product was created by 'stacking' these gridded surfaces to produce a dataset that defined, for each 50 m cell, the geological conditions at the nine specified depths. It was then a straightforward process to convert this dataset into one that had attributes defining 3D VCP values at specified depth intervals within this upper 20 m across the entire BGS London Lithoframe model. To ensure the compatibility of the GeoSure Shrink–Swell 3D product with the existing standard 2D GeoSure Shrink–Swell product, two additional attributes were added for each 50 m cell: the dominant (modal) VCP value and the range of the VCP values. The GeoSure Shrink–Swell 3D product provides GIS gridded maps for each of the 12 (20 × 20 km) squares; these display the VCP values at any of the specified depths (Fig. 22). Alternatively, a tabulation of the vertical distribution of VCP values for each 50 × 50 m cell can be requested (Table 5).

Conclusions

- 2D representations, based on statistical analyses, of the volume change potential (VCP) in the London Clay Formation (LC) show general trends. 3D models, such as those created by the S-Grid and facies techniques, provide a seamless interpolation and deliver a visualization of VCP that can be interpreted across a variety of depths.
- The calculated upper quartile (75th percentile) value of the modified plasticity index (I_P') across the entire onshore outcrop of the LC, Gault Formation (GLT) and Atherfield Clay Formation (AC) is indicative of a high VCP.
- The calculated upper quartile (75th percentile) value of I_P' across the entire onshore outcrop of the Lambeth Group

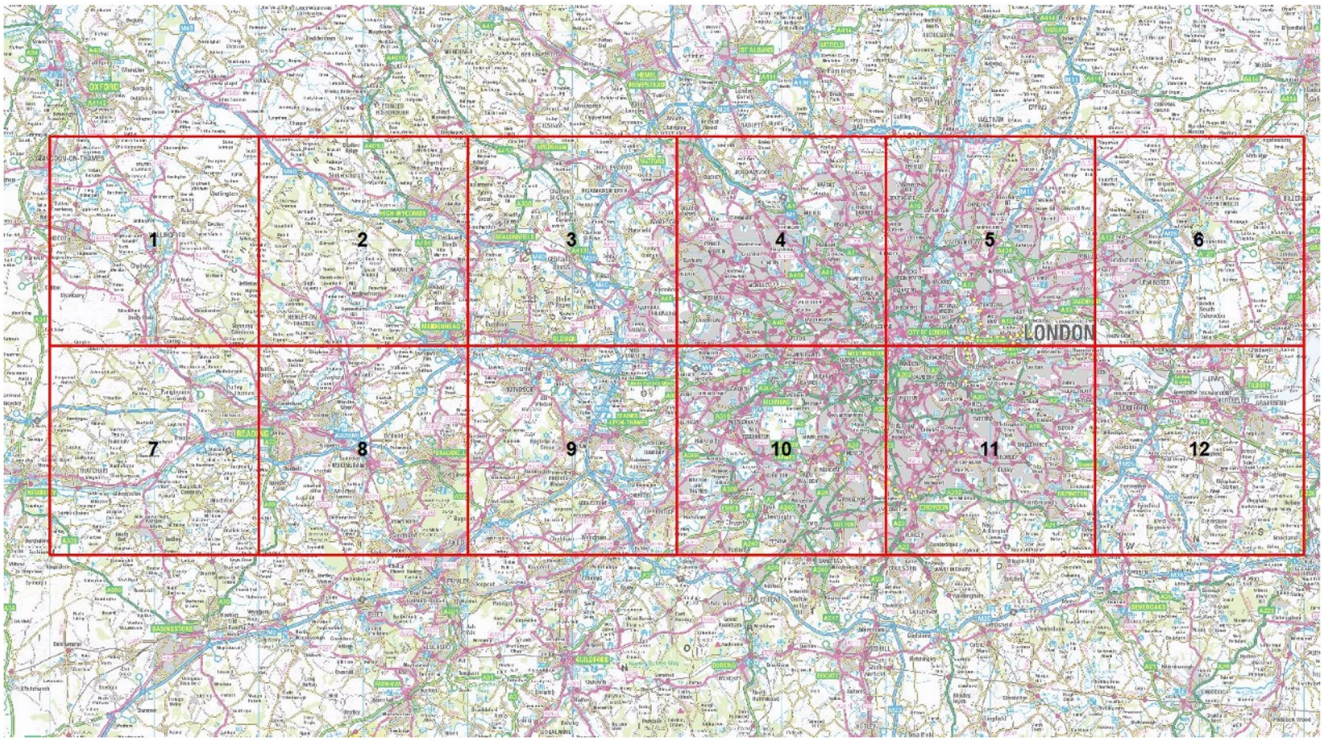

Fig. 21. Coverage of the Shrink–Swell 3D dataset. Source: contains Ordnance Survey data © Crown Copyright and database rights 2020.

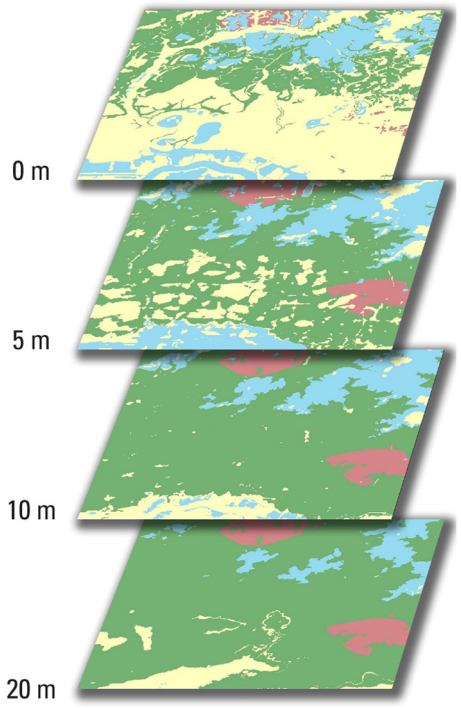

Fig. 22. Distribution of volume change potential (VCP) values at specified depths below ground within a 20 × 20 km square (yellow, low VCP; blue, medium VCP; green, high VCP; red, very high VCP).

Table 5. Example of GeoSure Shrink–Swell 3D tabulation for a 50 × 50 m cell

Depth (m bgl)	Formation code*	Dominant VCP ranking	Range of VCP rankings
0	MGR	A	
1	ALV	C	A–C
2	ALV	C	A–C
3	LASI	B	
4	LASI	B	
5	LC	D	A–E
10	LC	D	A–E
15	LC	D	A–E
20	LC	D	A–E

*MGR, made ground; ALV, alluvium; LASI, Langley Silt; LC, London Clay.

(LMBE), Lias Clay Formation (LIAS), Weald Clay Formation (WC), Oxford Clay Formation (OXC), Kimmeridge Clay Formation (KC) and Wadhurst Clay Formation (WDC) is indicative of a medium VCP.

- The calculated upper quartile (75th percentile) value of I_P' across the entire onshore outcrop of the Mercia Mudstone Group (MMG) is indicative of a low VCP.
- Both the statistical and spatial analyses confirm a west–east and a south–north trend of increasing plasticity and, hence, the VCP for the AC, LC and OXC.
- Both the statistical and spatial analyses confirm a west–east and a north–south trend of increasing plasticity and, hence, the VCP for the GLT. They also show an increase in plasticity with depth.
- Both the statistical and spatial analyses confirm a west–east only trend of increasing plasticity and, hence, VCP for the MMG.
- Both the statistical and spatial analyses confirm an east–west and a south–north trend of increasing plasticity and, hence, VCP for the WDC and WC.
- Both the statistical and spatial analyses confirm no trend of increasing (or decreasing) plasticity and, hence, VCP in any direction for the KC and LIAS.
- The statistical analysis confirms a slight east–west trend of increasing plasticity and, hence, VCP for the LMBE, but the spatial analysis showed no sign of this trend.

- 2D representations based on statistical analyses show general trends of increasing and/or decreasing VCP; but with large amounts of data unevenly spread over a wide area, the detail is lost.
- The inverse distance weighting (IDW) spatial modelling technique is affected by the data distribution, calling into question the validity of the predicted model. In effect, the output value can never be higher than the greatest value or less than the lowest value, whereas 3D models, such as those calculated by S-Grid, provide a seamless interpolation, giving a visualization that allows the I_P' values to be examined at a variety of depths relative to ground level.
- The London Clay Formation (LC): the results of the modelling have confirmed variations of the VCP with depth across central and east London and south Essex as follows:
  - near-surface: little variation, the VCP is high across the area;
  - 8–20 m: increasing plasticity east of London; around the mouth of the River Thames the VCP changes from high to very high;
  - 20–30 m: decrease in plasticity in central London (Area 3a) and the VCP changes from high to medium; plasticity remains the same in the east and the VCP is very high; and
  - >30 m (not shown): a decrease in plasticity in the east, and the VCP changes from very high to high. Plasticity remains the same in central London and the VCP is medium.
- Lithofacies (facies) modelling using S-Grids allows a more realistic representation of this type of physical properties data (I_P', VCP, bulk density, dry density, standard penetration tests etc.). It allows attributes to grade into each other, which better captures their interfingered nature and the variability of the subsurface.
- The main aim of the facies modelling was to show that VCP values can be used as a proxy to show the variability of shrinking and swelling clays, particularly along linear alignments, which is how much of the data was spatially distributed.
- Further studies would prove useful in determining how good these types of models are at demonstrating the 'true' nature of these types of physical property data along linear alignments. The potential of this work could save time and money for relevant businesses, especially those related to underground services and infrastructure, and where climate change influences these (Rotta Loria 2023).
- Further work could be undertaken in order to include bootstrapping techniques whereby proportions of the data are removed from the conditioning data and the simulation then re-run without that data and the results compared. This process would be repeated a number of times, allowing the user to quantify the reliability of predictions in the facies model.
- The Geovisionary software provides a means of viewing the facies-type generated data in a fully immersive 3D, or even 4D, environment. This type of environment lends itself to both education and research, as well as to visualization and modelling. Voxel models are easily imported and are able to be visualized in their 'true' spatial position, overlying geology or standard maps. The data values can be shown as sections using clipping planes in any direction, or specific data values can be extracted to show where these occur spatially in order to predict possible tendencies, or show actual trends in the data. It can be used in tandem with many other datasets to provide insights that you would not necessarily get from looking at the data in isolation in a modelling package.
- The GeoSure Shrink–Swell 3D model for London is part of the BGS GeoSure range of natural subsidence products. Based on data contained within the London Geological Model (Mathers *et al.* 2014), it provides a regional susceptibility model of potential shrink–swell hazard, in 3D, at intervals down to 20 m in the London and Thames Valley area.
- The Geosure Shrink–Swell 3D dataset provides an information resource for asset and infrastructure development and maintenance. The shrink–swell properties of the LC affect developers, construction companies and local government due to increased costs of insurance, additional engineering works to stabilize land or potential relocation of developments. Information on the 3D distribution of shrink–swell properties permits identification of potential problems at the surface, in the shallow subsurface or deeper underground.
- This type of modelling could be used for many applications in the construction industry, especially those relating to infrastructure developments and maintenance. These types of scenarios would lend themselves well to applications such as climate change and temperature anomalies in the ground beneath London (for example), and the thermal imprint of heat islands due to underground transport (including trains braking), residential basement and paving of previously open spaces (Bidarmaghz *et al.* 2020).

Scientific editing by Colin Joseph Serridge; Gareth Usher;

Acknowledgements This paper is published with the permission of the Executive Director of the British Geological Survey. The authors would like to thank Bruce Napier (British Geological Survey) and Pete Hobbs (British Geological Survey) for reviewing the paper.

Author contributions **LDJ**: conceptualization (lead), formal analysis (equal), investigation (lead), methodology (lead), writing – original draft (lead), writing – review & editing (lead); **RT**: formal analysis (equal), validation (equal), visualization (equal); **AH**: software (equal), validation (equal), visualization (equal).

Funding This research received funding from the Natural Environment Research Council (awarded to L.D. Jones).

Competing interests The authors declare that they have no known competing financial interests or personal relationships that could have appeared to influence the work reported in this paper.

Data availability The datasets generated during and/or analysed during the current study are available in the BGS repository: www.bgs.ac.uk

References

Bidarmaghz, A., Choudhary, R., Soga, K., Terrington, R., Kessler, H. and Thorpe, S. 2020. Large-scale urban underground hydro-thermal modelling – a case study of the Royal Borough of Kensington and Chelsea, London. *Science of the Total Environment*, **700**, https://doi.org/10.1016/j.scitotenv.2019.134955

BRE 1993*a*. *Low-Rise Buildings on Shrinkable Clay Soils: Parts 1, 2 and 3*. BRE Digest, **240, 241 and 242**. CRC Press, London.

BRE 1993*b*. *Low-Rise Buildings on Shrinkable Clay Soils: Part 1*. BRE Digest, **240**. Building Research Establishment (BRE), Watford, UK.

Cox, B.M., Hudson, J.D. and Martill, D.M. 1992. Lithostratigraphic nomenclature of the Oxford Clay (Jurassic). *Proceedings of the Geologists' Association*, **103**, 343–345, https://doi.org/10.1016/S0016-7878(08)80130-7

Cox, B.M., Sumbler, M.G. and Ivimey-Cook, H.C. 1999. *A Formational Framework for the Lower Jurassic of England and Wales (Onshore Area)*. BGS Research Report RR/99/01. British Geological Survey (BGS), Keyworth, Nottingham, UK.

Culshaw, M.G. 2005. From concept towards reality: developing the attributed 3D geological model of the shallow subsurface. *Quarterly Journal of Engineering Geology and Hydrogeology*, **38**, 231–284, https://doi.org/10.1144/1470-9236/04-072

Driscoll, R. 1983. The influence of vegetation on the swelling and shrinking of clay soils in Britain. *Geotechnikque*, **38**, 93–105, https://doi.org/10.1680/geot.1983.33.2.93

Driscoll R. and Crilly, M. 2000. *Subsidence Damage to Domestic Buildings. Lessons Learned and Questions Asked*. BRE Press, London.

Ellison, R.A., Knox, RWO'B, Jolley, D.W. and King, C. 1994. A revision of the lithostratigraphical classification of the early Palaeogene strata of the London Basin and East Anglia. *Proceedings of the Geologists Association*, **105**, 187–197, https://doi.org/10.1016/S0016-7878(08)80118-6

Forster, A., Hobbs, P.R.N. *et al.* 1994. *The Engineering Geology of British Rocks and Soils. The Gault Clay in England*. BGS Technical Report WN/94/31. British Geological Survey (BGS), Keyworth, Nottingham, UK.

Freeborough, K., Venus, J. and Kirkham, K. 2011. *Determination of the Shrinking and Swelling Properties of the Weald Clay Formation*. BGS Internal Report IR/11/035. British Geological Survey (BGS), Keyworth, Nottingham, UK.

Gallois, R.W. and Worssam, B.C. 1993. *Geology of the Country around Horsham. Memoir of the British Geological Survey, Sheet 302 (England and Wales)*. British Geological Survey (BGS), Keyworth, Nottingham, UK.

Hallam, J.R. 1990. *The Statistical Analysis and Summarisation of Geotechnical Databases*. BGS Technical Report WN/90/16. British Geological Survey (BGS), Keyworth, Nottingham, UK.

Harrison, A.M., Plim, J., Harrison, M., Jones, L.D. and Culshaw, M.G. 2012. The relationship between shrink–swell occurrence and climate in south-east England. *Proceedings of the Geologists' Association*, **123**, 556–575, https://doi.org/10.1016/j.pgeola.2012.05.002

Hobbs, P.R.N., Hallam, J.R. *et al.* 2002. *Engineering Geology of British Rocks and Soils: Mudstones of the Mercia Mudstone Group*. BGS Research Report RR/01/002. British Geological Survey (BGS), Keyworth, Nottingham, UK.

Hobbs, P.R.N., Entwisle, D.C. *et al.* 2012. *Engineering Geology of British Rocks and Soils: Lias Group*. BGS Open Report OR/12/032. British Geological Survey (BGS), Keyworth, Nottingham, UK.

Hopson, P.M., Farrant, A.R. and Booth, K.A. 2001. Lithostratigraphy and regional correlation of the basal Chalk, Upper Greensand, Gault and Uppermost Folkestone formations (Mid-Cretaceous) from cored boreholes near Selborne, Hampshire. *Proceedings of the Geologists' Association*, **112**, 193–210, https://doi.org/10.1016/S0016-7878(01)80001-8

Hopson, P.M., Wilkinson, I.P. and Woods, M.A. 2008. *A Stratigraphical Framework for the Lower Cretaceous of England*. BGS Research Report RR/08/03. British Geological Survey (BGS), Keyworth, Nottingham, UK.

Horton, A., Sumbler, M.G., Cox, B.M. and Ambrose, K. 1995. *Geology of the Country around Thame: Memoir of the British Geological Survey, Sheet 237 (England and Wales)*. British Geological Survey (BGS), Keyworth, Nottingham, UK.

Howard, A.S., Warrington, G., Ambrose, K. and Rees, J.G. 2008. *A Formational Framework for the Mercia Mudstone Group (Triassic) of England and Wales*. BGS Research Report RR/08/04. British Geological Survey (BGS), Keyworth, Nottingham, UK.

Intermap Technologies 2007. *NEXTMap British Digital Terrain Model Dataset Produced by Intermap*. National Centre for Earth Observation (NERC) Earth Observation Data Centre, Leicester, UK.

Jones, L.D. 2001. *Determination of the Shrinking and Swelling Properties of the Clays of the Lambeth Group*. BGS Internal Report IR/01/54. British Geological Survey (BGS), Keyworth, Nottingham, UK.

Jones, L.D. 2004. Cracking open the property market. *Planet Earth*. Autumn 2004, 30–31.

Jones, L.D. and Hobbs, P.R.N. 1998*a*. *The Shrinkage and Swelling Behaviour of UK Soils: Gault Clay*. BGS Technical Report WN/98/13. British Geological Survey (BGS), Keyworth, Nottingham, UK.

Jones, L.D. and Hobbs, P.R.N. 1998*b*. *The Shrinkage and Swelling Behaviour of UK Soils: Mercia Mudstone*. BGS Technical Report WN/98/14. British Geological Survey (BGS), Keyworth, Nottingham, UK.

Jones, L.D. and Hobbs, P.R.N. 2004. *The Shrinkage and Swelling Behaviour of UK Soils: Clays of the Lambeth Group*. BGS Research Report RR/04/01. British Geological Survey (BGS), Keyworth, Nottingham, UK.

Jones, L.D. and Jefferson, I. 2012. Expansive soils. *In*: Burland, J., Chapman, T., Skinner, H. and Brown, M. (eds) *ICE Manual of Geotechnical Engineering. Volume 1: Geotechnical Engineering Principles, Problematic Soils and Site Investigation*. ICE Publishing, London, 413–441.

Jones, L.D. and Terrington, R. 2011. Modelling volume change potential in the London Clay. *Quarterly Journal of Engineering Geology and Hydrogeology*, **44**, 1–15, https://doi.org/10.1144/1470-9236/08-112

Jones, L.D., Terrington, R. and Hulbert, A. 2017. *Methods for Modelling the 3D Volume Change Potential of UK Clay Soils*. BGS Research Report RR/17/008. British Geological Survey (BGS), Keyworth, Nottingham, UK.

Kearsey, T., Finlayson, A., Williamson, P., Williams, J.D.O., Terrington, R.L., Kingdon, A. and Campbell, S.D.G. 2011. Comparing and fusing deterministic and stochastic geological models: an example from the City of Glasgow, UK. Presented at the Model Fusion Conference, 28–29 November 2011, London, UK, http://nora.nerc.ac.uk/16001

Kearsey, T., Williams, J. *et al.* 2015. Testing the application and limitation of stochastic simulations to predict the lithology of glacial and fluvial deposits in Central Glasgow, UK. *Engineering Geology*, **187**, 98–112, https://doi.org/10.1016/j.enggeo.2014.12.017

Kessler, H., Mathers, S. and Sobisch, H.-G. 2009. The capture and dissemination of integrated 3D geospatial knowledge at the British Geological Survey using GSI3D software and methodology. *Computers & Geosciences*, **35**, 1311–1321, https://doi.org/10.1016/j.cageo.2008.04.005

King, C. 1981. *The Stratigraphy of the London Clay and Associated Deposits*. Tertiary Research Special Papers, **6**. W. Backhuys, Rotterdam, The Netherlands.

Lam, N.S.N. 1983. Spatial interpolation methods: A review. *The American Cartographer*, **10**, 129–149, https://doi.org/10.1559/152304083783914958

Lee, K.A. and Diaz Doce, D. 2017. *User Guide for the British Geological Survey GeoSure Dataset: Version 8*. BGS Open Report OR/17/050. British Geological Survey (BGS), Keyworth, Nottingham, UK.

Mathers, S.J., Burke, H.F., Terrington, R.L., Thorpe, S., Dearden, R.A., Williamson, J.P. and Ford, J.R. 2014. A geological model of London and the Thames Valley, Southeast England. *Proceedings of the Geologists' Association*, **125**, 373–382, https://doi.org/10.1016/j.pgeola.2014.09.001

Met Office 2018. United Kingdom Climate Predictions (UKCP). Met Office, Exeter, UK, https://www.metoffice.gov.uk/research/approach/collaboration/ukcp/index

Reeves, G.M., Sims, I. and Cripps, J.C. (eds) 2006. *Clay Materials Used in Construction*. Geological Society, London, Engineering Geology Special Publications, **21**, https://doi.org/10.1144/GSL.ENG.2006.021.01.21

Rotta Loria, A.F. 2023. The silent impact of underground climate change on civil infrastructure. *Communications Engineering*, **2**, 44, https://doi.org/10.1038/s44172-023-00092-1

Simpson, M.I. 1985. The stratigraphy of the Atherfield Clay Formation (Lower Aptian, Lower Cretaceous) at the type and other localities in southern England. *Proceedings of the Geologists' Association*, **96**, 23–45, https://doi.org/10.1016/S0016-7878(85)80012-2

Stafleu, J., Maljers, D. *et al.* 2012. *GeoTOP Modellering (in Dutch)*. TNO Report 2012 R10991. The Netherlands Organization for Applied Scientific Research (TNO), The Hague, The Netherlands.

Terrington, R., Napier, B., Buchi, A. and Procopio, P.M. 2015. Managing the mining cycle using GeoVisionary. Presented at the Aachan International 5th Mining Symposia, 27–28 May 2015, Aachan, Germany.

Walsby, J.C. 2008. GeoSure; a bridge between geology and decision-makers. *Geological Society, London, Special Publications*, **305**, 81–87, https://doi.org/10.1144/SP305.9

Woods, M.A., Newell, A.J., Haslam, R., Farrant, A.R. and Smith, H. 2015. *A Physical Property Model of the Chalk of Southern England*. BGS Open Report OR/15/013. British Geological Survey (BGS), Keyworth, Nottingham, UK.